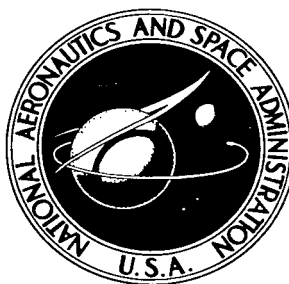


NASA TECHNICAL NOTE



NASA TN D-3980

e.1

NASA TN D-3980

**LOAN COPY: RETURN
AFWL (WJL-2)
KIRTLAND AFB, N M**

0131026



TECH LIBRARY KAFB, NM

**DYNAMIC MODEL INVESTIGATION OF
WATER PRESSURES AND ACCELERATIONS
ENCOUNTERED DURING LANDINGS
OF THE APOLLO SPACECRAFT**

by Sandy M. Stubbs

Langley Research Center

Langley Station, Hampton, Va.



DYNAMIC MODEL INVESTIGATION OF WATER PRESSURES
AND ACCELERATIONS ENCOUNTERED DURING
LANDINGS OF THE APOLLO SPACECRAFT

By Sandy M. Stubbs

Langley Research Center
Langley Station, Hampton, Va.

Technical Film Supplement L-960 available on request.

NATIONAL AERONAUTICS AND SPACE ADMINISTRATION

For sale by the Clearinghouse for Federal Scientific and Technical Information
Springfield, Virginia 22151 - CFSTI price \$3.00

DYNAMIC MODEL INVESTIGATION OF WATER PRESSURES
AND ACCELERATIONS ENCOUNTERED DURING
LANDINGS OF THE APOLLO SPACECRAFT

By Sandy M. Stubbs
Langley Research Center

SUMMARY

An experimental investigation was made to determine impact water pressures, accelerations, and landing dynamics of a 1/4-scale dynamic model of the command module of the Apollo spacecraft. A scaled-stiffness aft heat shield was used on the model to simulate the structural deflections of the full-scale heat shield. Tests were made on water to obtain impact pressure data at a simulated parachute letdown (vertical) velocity component of approximately 30 ft/sec (9.1 m/sec) full scale. Additional tests were made on water, sand, and hard clay-gravel landing surfaces at simulated vertical velocity components of 23 ft/sec (7.0 m/sec) full scale. Horizontal velocity components investigated ranged from 0 to 50 ft/sec (15 m/sec) full scale and the pitch attitudes ranged from -40° to 29° . Roll attitudes were 0° , 90° , and 180° , and the yaw attitude was 0° .

Results indicated that maximum mean water pressures on sample panel areas of the vehicle aft heat shield (areas of approximately 2 ft² (0.2 m²)) were about 214 psi (1475 kN/m²) full scale. The mean pressure at the time of maximum acceleration was approximately 60 psi (414 kN/m²) over a heat-shield area of about 20 ft² (1.9 m²) full scale. Maximum normal, longitudinal, and angular accelerations for the 30 ft/sec (9.1 m/sec) vertical velocity on water were 38g, 7.5g, and 180 rad/sec², respectively (1g = 9.8 m/sec²). Normal accelerations for water landings showed pronounced oscillations due to heat-shield vibration, and the 38g maximum acceleration is higher than that expected from a rigid vehicle. The vehicle occasionally turned over for landings in water at a 0° roll attitude. The roll axis is an axis parallel to the axis of geometric symmetry. The 180° roll attitude gave much improved stability with no turnover. The vehicle was found to float stably in an upright as well as in a near inverted attitude. Waves 2 feet (0.6 m) high and 36 feet (11 m) long (full scale) failed to upset the vehicle from either flotation position.

Additional landings investigated on water, sand, and hard clay-gravel composite surfaces resulted in maximum normal accelerations of 30g, 49g, and 42.5g, respectively. Heat-shield failure occurred for all tests but one made on sand and for all tests made on the hard clay-gravel landing surfaces.

INTRODUCTION

The landing characteristics of various models of manned spacecraft have been investigated by the National Aeronautics and Space Administration and are presented in references 1 to 5. The Apollo command module is currently being developed for a three-man lunar mission which includes an earth landing by parachute. The original landing system design for the Apollo spacecraft called for a deployed heat shield with the landing media being soil (primary) and water (secondary). For various reasons, these criteria were changed after the development of the landing system was underway. The landing system was changed to a passive system (landing system that does not require heat-shield deployment or braking rockets) with water as the primary landing media and soil secondary. The present investigation was begun at the onset of the change to water as the primary landing media.

The purpose of the present investigation was to determine the impact pressures and accelerations imposed on a 1/4-scale dynamic model of the Apollo command module for landings on water at conditions simulating parachute letdown. The heat-shield stiffness was scaled from an early Apollo heat-shield structural design. (See ref. 6.) The investigation was conducted in order to obtain water impact loads for design purposes. In addition to water landings, a brief investigation was conducted to determine the accelerations and landing characteristics of a spacecraft for landings on sand and hard clay-gravel composite surfaces. The investigations were conducted in the Langley impacting structures facility.

The units used for the physical quantities defined in this report are given both in U.S. Customary Units and in the International System of Units (SI). (See ref. 7.) Appendix A presents factors relating these two systems of units. All test conditions and results are presented in full-scale values unless otherwise indicated.

DESCRIPTION OF MODEL

The model used in the investigation was a 1/4-scale dynamic model of the Apollo spacecraft. The scale relationships used in the investigation are shown in table I. Pertinent parameters of the model and full-scale vehicle are given in table II.

Dimensions of the prototype Apollo spacecraft from which the model was scaled are shown in figure 1. Photographs of the model are shown in figure 2. Model construction details are shown in figure 3. The heat shield was held in place against a support ring on the model by four turnbuckles. The aft bulkhead that is located immediately behind the heat shield in the full-scale spacecraft was not simulated in the model investigation. The model was constructed with balsa wood and mahogany blocks and was covered with

several layers of fiber glass. Mahogany was used where hard points were needed, such as around the heat-shield support ring and at the turnbuckle attachment points. Accelerometers were mounted on solid mahogany blocks and were accessible through holes left in the balsa wood.

The construction details of the heat shield used with the passive landing system are shown in figure 4. The heat-shield stiffness was scaled from an early Apollo heat-shield structural design (see ref. 6) but the failure strength was not scaled. For the model, a sandwich construction was used with a core of styrene plastic covered on each side by two layers of glass cloth impregnated with an epoxy resin. Lead weights were distributed between the fiber-glass layers on 2-inch (5-cm) centers (model scale) to obtain the proper inertia characteristics of the heat shield. The deflection of the model-scale heat shields was determined from compression tests using the 1 200 000-pound-capacity universal static hydraulic testing machine at the Langley Research Center shown in figure 5. The load deflection curve of the heat shield used in the present investigation (heat shield 28) is presented in figure 6 along with a curve of the loading of a typical heat shield (heat shield 20) through its failure regime. The deflection presented was measured from the movement of the machine head (fig. 5).

The locations of pressure transducers on the heat shield are shown in figure 7. The pressure transducers were located in groups of three in an attempt to obtain mean pressures from arbitrary circular panel areas A, B, C, D, and E. (See appendix B for the definition of mean pressure.) Each panel represented an area of approximately 2 ft² (0.2 m²) full scale and was only a designated finite area on the heat shield, not a structural element.

APPARATUS AND PROCEDURE

Test Conditions

The model was landed on water, sand, and hard clay-gravel composite surfaces. Tests made on the water landing surface simulated parachute letdown (vertical) velocity components from 21 to 36 ft/sec (6.4 to 11 m/sec) full scale. Landings made on the sand and the hard clay-gravel surfaces simulated a vertical velocity component of 23 ft/sec (7.0 m/sec). Horizontal velocity components for landings on water ranged from 0 to 50 ft/sec (15 m/sec) full scale. Landings on sand were made with no horizontal velocity component and landings on the hard clay-gravel surface were made with a horizontal velocity component of 30 ft/sec (9.1 m/sec) only. Landing attitudes ranged from -41° to 29°, and roll attitudes of 0°, 90°, and 180° were investigated. Figure 8 shows the model acceleration axes, flight path, force directions, and landing attitudes.

It should be noted that the definitions of roll and yaw axes are different from those of the standard aircraft axes.

The water landing tests were made in calm fresh water. The sand used for sand landings was dry Standard Ottawa Testing Sand. It was not meant to represent any particular terrain but was chosen because its controlled uniform characteristics favor reproducible experiments. The composite material used for the hard surface landings was a clay-gravel mixture that was moistened and rolled smooth as it was being installed. After rolling it smooth, it was allowed to dry to a hard surface before testing began. The coefficient of sliding friction between the fiber-glass heat shield and the clay-gravel composite surface was approximately 0.35.

Initial tests were made on water to obtain impact water pressures and accelerations. Subsequently, additional landing tests, made on water, sand, and the hard clay-gravel composite surfaces, were conducted to obtain only acceleration data. For the water pressure investigation, it was assumed that the spacecraft would be hung under the parachute at a -26° pitch attitude. A variation in landing pitch attitude from -10° to -42° was tested to include the swing (up to $\pm 8^{\circ}$) of the spacecraft about the parachute letdown attitude of -26° in addition to possible wave slopes (up to $\pm 8^{\circ}$).

For the additional landing tests made to obtain only acceleration data, it was assumed that the spacecraft would be hung under the parachute at a -10° pitch attitude. This assumption is based on results of hard-surface landings presented in reference 8 which indicate that negative pitch landing attitudes are more stable than positive pitch attitudes for landings at 0° roll on land. A variation in pitch attitude from -30° to 29° was tested to simulate spacecraft swing and wave slope. All tests were conducted at 0° yaw. Roll attitudes of 0° , 90° , and 180° were investigated.

Launch Procedure and Apparatus

A sketch showing the launch procedure is given in figure 9. A pendulum was released from a predetermined height to produce the desired horizontal velocity. The model was released at the lowest point of the swing, and the free fall gave the desired vertical velocity. A photograph of the launch apparatus for landings on water is shown in figure 10. Motion pictures were made to record the landing behavior of the model.

Flotation stability investigations were made by using an oscillating-type of wave maker to produce a train of waves 2 feet (0.61 m) high by 36 feet (11 m) long (full scale).

Instrumentation

Normal, longitudinal, and transverse accelerations were measured at the center of gravity of the vehicle by using linear strain-gage accelerometers. Angular (pitch)

accelerations were measured with matched pairs of linear accelerometers. Signals from the accelerometers were transmitted through trailing cables to the recording equipment. The response characteristics of the accelerometers and related recording equipment (amplifier, oscillograph, and galvanometers) are given in table III.

Impact water pressures were measured with strain-gage pressure transducers. The response characteristics of the transducers and recording equipment are shown in table III. The transducers had a 0.50-inch (1.3-cm) diameter diaphragm and were flush mounted in the heat shield. A thin plastic tape was placed over the diaphragm of each transducer to insulate it from the temperature shock that occurs upon contact with the water. It was determined that the tape did not affect the pressure values but acted only as an insulator.

RESULTS AND DISCUSSION

The data obtained in the investigation are presented in tables IV, V, VI, and VII, but only selected conditions (in general, those that have quantities of data and show definite trends) are plotted and discussed. All values presented in this section are full scale unless otherwise indicated.

A motion-picture film supplement (L-960) showing landing tests of the 1/4-scale model of the Apollo command module made on water, sand, and hard clay-gravel composite surfaces has been prepared and is available on loan. A request card form will be found at the back of this report.

Water Pressure Investigation

Typical oscillograph records obtained in the water pressure investigation are shown in figure 11. Figure 11(a) shows data for a pitch attitude of -11° , figure 11(b) is for a pitch attitude of -21° , and figure 11(c) is for a pitch attitude of -38° . The vertical and horizontal velocity components at impact were both 30 ft/sec (9.1 m/sec). Roll and yaw attitudes were 0° . The dashed lines are fairings of the accelerometer and pressure transducer traces. Data presented in tables IV to VII and in the data figures were obtained from similar fairings.

Acceleration data obtained in water pressure investigation.- The normal acceleration traces in figure 11(a) show a major structural oscillation (dashed line) which occurs because of the vibration of the flexible heat shield. (In tests of a model with a rigid heat shield, not reported herein, the low frequency oscillation does not occur.) This oscillation decreases as the pitch attitude is increased (see fig. 11(b)) until it is no longer pronounced (see fig. 11(c)).

Maximum acceleration data for the water pressure investigation are shown in figure 12 for the three horizontal velocities tested. The vertical velocity for this investigation varied from 29.2 to 32.4 ft/sec (8.90 to 9.88 m/sec). The open symbols indicate that the vehicle came to rest in the water floating in an upright attitude. The shaded data points indicate that turnover occurred. The normal acceleration for a 0° roll attitude (fig. 12(a)) varied from about 4g at a -39° attitude to 38g at a -12° landing attitude. Theoretical accelerations computed by using the procedure presented in reference 1 for a rigid vehicle gave a maximum normal acceleration of approximately 22g for a 0° attitude and a vertical velocity of 30 ft/sec (9.1 m/sec). The higher values of acceleration obtained in the experimental investigation are due to the structural oscillations of the flexible heat shield. It is possible, therefore, that a full-scale spacecraft with a flexible heat shield can experience greater structural loads than would be predicted from rigid-model theory. Horizontal velocity changes had little effect on maximum normal accelerations. The longitudinal accelerations increased as the landing attitude was varied from -39° to -11° . The maximum longitudinal acceleration was 7.5g and occurred at an attitude of -12° . A noticeable effect of horizontal velocity on longitudinal accelerations occurred for landing attitudes from -39° to -26° but little effect was noted at the other attitudes investigated. The angular accelerations varied from approximately 30 rad/sec² at a landing attitude of -39° to about 170 rad/sec² at -12° .

Maximum acceleration data for the water pressure investigation for the 180° roll attitude is shown in figure 12(b). These accelerations were similar to those at 0° roll. (See fig. 12(a).) However, for the 180° roll attitude, the stability was improved to the point that all runs ended with the vehicle floating in an upright attitude.

Pressure data.- The method of interpreting the data for the individual panels to obtain the mean pressure is illustrated in figure 13 and discussed in appendix B. The results from the analysis of the panel pressure data are shown in figure 14. Data obtained at 0° roll attitudes are presented in figure 14(a) and data obtained at 180° roll are presented in figure 14(b). For the 0° roll condition (fig. 14(a)) the mean pressure on panel A increased from about 30 psi (205 kN/m²) at a pitch attitude of -39° to 214 psi (1475 kN/m²) at a -18° attitude and then decreased to 95 psi (655 kN/m²) at an attitude of -11° . The impact water pressure experienced by a panel is dependent on the impacting velocity and on the angle at which the panel strikes the water. Panel A contacted the water at a near zero, or flat, attitude when the vehicle was at a pitch attitude of -18° . (See fig. 7.) For angles greater than -18° (such as -39°), panel A was the first panel to contact the water and thus should have higher pressures than the other panels. However, the attitude at which it struck the water was increasing so that at a pitch attitude of -39° the panel was at a 21° angle with respect to the water surface. The increasing panel contact angle resulted in the decreasing pressures for landing attitudes from -18° to -39° .

Panel B impacted the water at a flat angle for a -11° landing attitude. At this attitude the maximum mean pressure for panel B, 155 psi (1070 kN/m^2), was less than the maximum value for panel A. It is thought that the reduction in maximum mean pressure might be due to the flexible heat shield backing away from the load. Panel C was located so that it would experience a flat impact at a vehicle attitude of about -3° . Since the lowest angle tested was -11° , panel C would be expected to have its maximum pressure at this attitude and this value was approximately 110 psi (760 kN/m^2). The vehicle was tested at such angles that panels D and E like C never experienced a flat impact. For this reason the pressures on these panels were lower than pressures on panels A and B.

The mean wetted-area pressure at the time of the maximum acceleration is also shown in figure 14. The method used to obtain the mean wetted-area pressure is discussed in appendix B. For the 0° roll condition (fig. 14(a)), the wetted area involved at the time of maximum acceleration varied from approximately 23 ft^2 (2.14 m^2) at a -11° pitch attitude to 4.1 ft^2 (0.38 m^2) at a -38° attitude. The total projected area of the aft heat shield was 125.2 ft^2 (11.63 m^2). The mean wetted-area pressure varied from 15 psi (103 kN/m^2) at a landing attitude of -39° to approximately 50 psi (345 kN/m^2) at a -11° attitude with occasional mean wetted-area pressures as high as 60 psi (414 kN/m^2) over a heat-shield area of approximately 20 ft^2 (1.9 m^2). It should be noted that the mean wetted-area pressure presented depends on the magnitude of the acceleration which is a function of the heat-shield stiffness or flexibility. Because the heat shield vibrated under the imposed load, there were oscillations in the amplitudes of the accelerations. (See faired curves of fig. 11(a).) The maximum acceleration was determined from the faired curves through the normal acceleration and longitudinal acceleration traces. A change in the heat-shield stiffness will change the acceleration magnitude because of the vibration of the heat shield under the applied load and also because of the heat-shield vibration changing the heat-shield shape and thus affecting the applied load itself.

Horizontal velocity has little effect on the panel pressures or on the mean wetted-area pressure at maximum acceleration. Representative scatter in the data (fig. 14(b)) can be seen in the three data points presented at the -20° landing attitude. The scatter can be attributed to ripples on the water surface, inaccuracies in flush mounting the gages, pressure gage reading errors, variations in data fairing, or in instrumentation response variations. However, even though there is scatter in the data, the overall results indicate definite pressure trends.

Figure 14(b) presents pressure data for the 180° roll condition. The trends of the data and the magnitude of the panel pressures and mean pressure at the time of maximum acceleration are similar to those experienced at the 0° roll condition (fig. 14(a)).

Investigation of Landings on Water, Sand, and Hard Clay-Gravel Landing Surfaces

Additional landing tests were made on water, sand, and hard clay-gravel composite landing surfaces. The purpose of these investigations was to obtain impact accelerations and landing dynamics. No water pressure measurements were made for the water landings presented in this section. Typical oscillograph records of accelerations for landings on water, sand, and hard clay-gravel composite landing surfaces are shown in figure 15. The oscillograph records are presented for test conditions simulating a vertical velocity of 23 ft/sec (7.0 m/sec), a -10° pitch attitude, and 0° roll and yaw attitudes.

Water landing surface.- The data shown in figure 15(a) are for landings on calm water at a horizontal velocity of 30 ft/sec (9.1 m/sec). The oscillations in the normal acceleration trace are similar to those shown earlier (fig. 11) for a vertical velocity of 30 ft/sec (9.1 m/sec). The magnitude of the acceleration is reduced, however, because of the lower vertical velocity (23 ft/sec (7.0 m/sec)). Figure 16(a) is a plot of acceleration data for a range of landing attitudes from -30° to 29° . The shaded data points again indicate turnover. The maximum normal accelerations varied from approximately 4g at the landing attitude extremes to 30g near the 0° attitude. Longitudinal accelerations gave positive and negative values for landing attitudes from -4° to 10° . The maximum longitudinal acceleration for all attitudes was 7g at a -10° attitude. Angular accelerations also had positive and negative values. The maximum angular acceleration was 140 rad/sec². It should be noted that some of the tables contain data not shown on the figures. Table V, for example, has limited data for roll attitudes of 90° and 180° .

Sand landing surface.- Figure 15(b) shows a typical oscillograph record of a landing on a sand surface at a zero horizontal velocity. Acceleration data for sand landings are presented in figure 16(b). Heat-shield failure occurred for the 0° and -5° attitude landings on sand. The landing at a -10° attitude did not produce a notable failure. The maximum normal acceleration was 49g and occurred at a 0° landing attitude. The maximum longitudinal acceleration occurred at -10° and was 13g. The maximum angular acceleration was 130 rad/sec² at a -10° attitude. If tests had been made at larger negative landing attitudes, it is expected that the normal acceleration would have decreased from the values shown and the longitudinal and angular accelerations would have increased.

Hard clay-gravel landing surface.- For landings on the hard clay-gravel composite surface, a typical oscillograph record is shown in figure 15(c) for a 30 ft/sec (9.1 m/sec) horizontal velocity. The normal acceleration trace has no major oscillations. Figure 16(c) shows acceleration data for four landings made on the hard clay-gravel surface. The testing was limited because of the failure of a heat shield on each run. Maximum normal accelerations were 42.5g for both the -10° and -20° landing attitudes.

The maximum longitudinal acceleration was 35g at a -20° attitude. Angular acceleration was a maximum at -30° and was 640 rad/sec^2 . All tests resulted in violent turnovers. Accelerations during the turnover are not presented because the upper structure of the model was extremely stiff and gave higher accelerations during turnover than would be expected on the prototype spacecraft.

Flotation

The brief flotation investigation conducted with the 1/4-scale model was done with an external volume added to the top of the vehicle to simulate the buoyancy effects of the spacecraft airlock (removed during the landing tests to facilitate attachment of the model to the launch apparatus). The vehicle has two stable flotation positions, near upright and on its side and top. When the vehicle turned over during a landing it did not return to an upright attitude. A photograph of the two stable flotation positions is shown in figure 17. Flotation tests made in waves 2 feet (0.61 m) high and 36 feet (11 m) long (full scale) showed that the vehicle rode well in the waves in the upright and also the inverted positions. The size wave investigated failed to upset the vehicle from either flotation position.

CONCLUDING REMARKS

Landing tests have been made with a 1/4-scale dynamic model of the Apollo command module having a scaled-stiffness aft heat shield to determine the impact water pressures, accelerations, and landing dynamics for landings on water, sand, and hard clay-gravel surfaces.

The model investigation indicated that maximum water pressures, on sample panel areas of the spacecraft heat shield (approximately 2 ft^2 (0.2 m^2) in area), were approximately 214 psi (1475 kN/m^2) at a vertical velocity of about 30 ft/sec (9.1 m/sec) (full scale). The maximum pressure at the time of maximum acceleration was approximately 60 psi (414 kN/m^2) over a heat-shield area of approximately 20 ft^2 (1.9 m^2). Maximum normal, longitudinal, and angular accelerations for the 30 ft/sec (9.1 m/sec) vertical landing velocity on water were approximately 38g, 7.5g, and 180 rad/sec^2 , respectively. The normal accelerations for water landings showed pronounced oscillations due to heat-shield vibration, and the maximum acceleration of 38g is higher than would be expected from a rigid vehicle. The vehicle occasionally turned over for 0° roll attitude landings in water. The 180° roll attitude gave much improved stability with no turnover.

Additional landings investigated on water, sand, and hard clay-gravel composite surfaces were made with a vertical velocity of 23 ft/sec (7.0 m/sec). Results indicate

that maximum normal accelerations for water landings were 30g. Landings on the sand surface gave maximum accelerations of 49g, and the hard clay-gravel surface gave maximum accelerations of 42.5g. Heat-shield failure occurred for all tests but one made on sand and for all tests made on the hard clay-gravel landing surfaces. The vehicle turned over for all tests made on the hard clay-gravel landing surface.

The vehicle was found to float stably in an approximately upright attitude as well as in a near inverted position. Waves, 2 ft (0.61 m) high and 36 ft (11 m) long, failed to upset the vehicle from either flotation position.

Langley Research Center,

National Aeronautics and Space Administration,

Langley Station, Hampton, Va., April 24, 1967,

124-08-04-06-23.

APPENDIX A

CONVERSION OF U.S. CUSTOMARY UNITS TO SI UNITS

The International System of Units (SI) was adopted by the Eleventh General Conference on Weights and Measures, Paris, October 1960, in Resolution No. 12 (ref. 7). Conversion factors for the units used herein are given in the following table:

Physical quantity	U.S. Customary Unit	Conversion factor (*)	SI Unit
Length	in.	0.0254	meters (m)
Area	in ²	6.4516×10^{-4}	meters ² (m ²)
Mass	slug	14.5939	kilograms (kg)
Moment of inertia	slug ft ²	1.35582	kilogram meters ² (kg m ²)
Velocity	ft/sec	0.3048	meters/second (m/sec)
Linear acceleration	ft/sec ²	0.3048	meters/second ² (m/sec ²)
Force	lbf	4.448	newtons (N)
Pressure	lbf/in ²	6.895×10^3	newtons/meter ² (N/m ²)

*Multiply value given in U.S. Customary Unit by conversion factor to obtain equivalent value in SI unit.

Prefixes to indicate multiples of units are as follows:

Prefix	Multiple
milli (m)	10^{-3}
centi (c)	10^{-2}
kilo (k)	10^3

APPENDIX B

PRESSURE DATA ANALYSIS

The approximate mean pressures presented in this report refer to sample panel areas A, B, C, D, and E each having an area of approximately 2 ft² (0.2 m²) full scale. The theoretical mean pressure is defined as the integration of the pressure over any one of the panels A, B, C, D, or E divided by the area of the panel, that is

$$p_m = \frac{1}{A} \int p \, dA$$

where

p_m mean pressure, psi (kN/m²)

p pressure, psi (kN/m²)

A panel area, in² (m²)

The preceding is the ideal method of obtaining the mean pressure; however, because of inaccuracies in instrumentation response, heat-shield flexibility, and so forth, the mean pressure was only approximated by two methods. One method used was an integrated panel pressure and the other was a simple arithmetic averaging of the three transducer values.

Figure 13 shows three sketches, panels A, B, and C drawn along the Z-axis. Only three transducers were used for each panel because of limited availability of instrumentation. The pressures presented for the panels are an approximate mean pressure loading of the panel obtained when the last transducer in the panel reached its maximum value. The point of initial contact is shown and the direction of the water line in moving across each panel is indicated by the arrowed line passing through the center of each panel. All three pressure transducers for a given panel (6, 7, and 8 for panel A) were read at the time that the last of the three transducers reached its peak value. The three pressure values for each panel are shown (fig. 13) as a function of the projected distance between the transducers; a dashed line indicates the fairing of the pressure diagram. The pressure diagram occurs along the solid line passing through the center of each panel (A-A, B-B, and C-C). Furthermore, the mean pressure value obtained from the diagram is considered to approximate the mean pressure over the entire panel.

APPENDIX B

For panel A the pressure diagram was integrated by dividing the diagram into four increments a, b, c, and d. The sum of the average values for the increments was divided by 4 to obtain the mean pressure for the panel. In general, panels were integrated when they were located with respect to the point of initial contact such that two transducers were read when both were at or near their peak pressure value. For panels that were not integrated (B and C are typical examples), a simple arithmetic average was used to approximate the mean pressure for the panel. The integrated method is a more accurate method of obtaining the mean pressure, but it is extremely more time consuming, and because of other inaccuracies in instrumentation response, heat-shield flexibility effect, water surface irregularities, and so forth, a simple averaging on most panels was considered adequate.

The mean wetted-area pressure over the wetted area at the time of maximum acceleration was determined in addition to the panel pressures. The pressure transducers in this case were used only to determine the position of the water line at the time of maximum acceleration. The wetted area was calculated by drawing the water line on a planform sketch of the heat shield and integrating with a planimeter. The mean wetted-area pressure was obtained from

$$p_{m,wa} = \frac{F}{A_w}$$

where $F = ma_r$ and

$p_{m,wa}$ mean wetted-area pressure, psi (kN/m²)

F force, lbf (N)

A_w wetted area, in² (m²)

m mass, slugs (kg)

a_r maximum resultant acceleration, ft/sec² (m/sec²)

It was difficult, however, to be sure of the exact time at which maximum acceleration was reached especially for the higher negative attitudes tested (fig. 11(c)). Therefore, the data presented for the mean wetted-area pressure at the time of maximum acceleration should be considered approximate.

REFERENCES

1. McGehee, John R.; Hathaway, Melvin E.; and Vaughan, Victor L., Jr.: Water-Landing Characteristics of a Reentry Capsule. NASA MEMO 5-23-59L, 1959.
2. Vaughan, Victor L., Jr.: Landing Characteristics and Flotation Properties of a Reentry Capsule. NASA TN D-653, 1961.
3. Stubbs, Sandy M.: Landing Characteristics of a Reentry Vehicle With a Passive Landing System for Impact Alleviation. NASA TN D-2035, 1964.
4. Thompson, William C.: Dynamic Model Investigation of the Landing Characteristics of a Manned Spacecraft. NASA TN D-2497, 1965.
5. Stubbs, Sandy M.: Landing Characteristics of the Apollo Spacecraft With Deployed-Heat-Shield Impact Attenuation Systems. NASA TN D-3059, 1966.
6. Bennett, R. V.; and Koerner, F. W.: 1/4 Scale Apollo Impact Attenuation Model. Rept. No. NA62H-513, North Am. Aviation, Inc., Sept. 14, 1962.
7. Mechtly, E. A.: The International System of Units - Physical Constants and Conversion Factors. NASA SP-7012, 1964.
8. Stubbs, Sandy M.: Investigation of the Skid-Rocker Landing Characteristics of Spacecraft Models. NASA TN D-1624, 1963.

TABLE I.- SCALE RELATIONSHIPS

$[\lambda = \text{Scale of model} = 1/4]$

Quantity	Full-scale value	Scale factor	Model value
Length	l	λ	λl
Area	A	λ^2	$\lambda^2 A$
Mass	m	λ^3	$\lambda^3 m$
Moment of inertia	I	λ^5	$\lambda^5 I$
Time	t	$\sqrt{\lambda}$	$\sqrt{\lambda} t$
Velocity	v	$\sqrt{\lambda}$	$\sqrt{\lambda} v$
Linear acceleration	a	1	a
Angular acceleration	α	λ^{-1}	$\lambda^{-1} \alpha$
Force	F	λ^3	$\lambda^3 F$
Pressure	p	λ	λp
Spring constant	k	λ^2	$\lambda^2 k$

TABLE II.- PERTINENT MEASURED PARAMETERS OF THE 1/4-SCALE MODEL
USED IN WATER PRESSURE INVESTIGATION

Parameter	1/4-scale model		Full-scale vehicle	
Mass	4.18 slugs	60.96 kg	267.3 slugs	3900 kg
Moment of inertia:				
I_x (roll)	4.01 slug ft ²	5.44 kg m ²	4100 slug ft ²	5560 kg m ²
I_y (pitch)	3.80 slug ft ²	5.14 kg m ²	3890 slug ft ²	5270 kg m ²
I_z (yaw)	3.01 slug ft ²	4.08 kg m ²	3080 slug ft ²	4180 kg m ²
Body:				
Diameter	37.88 in.	0.962 m	151.5 in.	3.85 m
Height	21.50 in.	0.546 m	86.20 in.	2.19 m
Landing velocity:				
Vertical (approximate) . . .	15 ft/sec	4.6 m/sec	30 ft/sec	9.1 m/sec
Horizontal	0 to 25 ft/sec	0 to 7.6 m/sec	0 to 50 ft/sec	0 to 15 m/sec

TABLE III.- ACTUAL INSTRUMENTATION CHARACTERISTICS

Accelerometer orientation	Range, g units	Natural frequency, cps	Damping, percent of critical damping	Limiting flat frequency of other recording equipment, cps
Normal (at vehicle c.g.)	±100	701	60	600
Longitudinal (at vehicle c.g.) ..	±50	633	70	600
Angular (pitch)	±200	1050	45	600
Transverse (at vehicle c.g.) ..	±50	613	55	600

Pressure transducer	Range		Approximate natural frequency in air, cps	Limiting flat frequency of other recording equipment, cps
	psi	kN/m ²		
6	100	690	11 000	6000
7	50	345	9 000	6000
8	50	345	9 000	6000
9	50	345	9 000	6000
10	50	345	9 000	6000
11	50	345	9 000	6000
12	50	345	9 000	6000
13	50	345	9 000	6000
14	50	345	9 000	6000
15	50	345	9 000	6000
16	50	345	9 000	6000
17	50	345	9 000	6000
18	50	345	9 000	5000
19	50	345	9 000	5000
20	50	345	9 000	5000

TABLE IV.- MAXIMUM ACCELERATION AND PRESSURE PANEL DATA FOR LANDINGS ON WATER

[All values are full scale]

Vertical velocity		Horizontal velocity		Landing attitude			Normal acceleration at c.g., g units	Longitudinal acceleration at c.g., g units	Angular acceleration, rad/sec ²	Vehicle mass		Mean pressure										Wetted area at time of maximum acceleration		Mean pressure at time of maximum acceleration		Stability			
ft/sec	m/sec	ft/sec	m/sec	Pitch, deg	Roll, deg	Yaw, deg				slug	kg	Panel A		Panel B		Panel C		Panel D		Panel E		in ²	m ²	psi	KN/m ²	Stable	Turnover		
32.4	9.88	0	0	-12	0	0	33.5	5.9	168	267.3	3901	101	696	*108	745	111	765	89	614	45	310	6640	4.284	42	290	✓			
31.8	9.69	0	0	-14	0	0	31.1	6.3	155			*144	993	89	614	113	779	*72	496			5260	3.394	48	331	✓			
32.0	9.75	0	0	-17	0	0	23.9	4.8	154			214	1475	*89	614	110	758	78	548	30	207	4980	3.213	40	276	✓			
31.4	9.57	0	0	-18	0	0	19.7	6.2	97			*120	827	*112	772	59	407	60	414	8	55	4290	2.768	30	207	✓			
31.7	9.66	0	0	-20	0	0	15.4	5.6	112			*136	938	115	793	27	186	57	393	10	69	3630	2.342	38	262	✓			
31.6	9.63	0	0	-20	0	0	13.9	5.1	97			*180	1241	*100	689	23	159	48	331	14	97	2800	1.806	45	310	✓			
31.6	9.63	0	0	-20	0	0	15.1	4.7	98			*152	1048	*92	634	36	248	50	345	10	69	3060	1.974	43	296	✓			
31.0	9.45	0	0	-22	0	0	15.6	6.8	92			*160	1103	80	552	27	186	34	234	14	97	2190	1.413	62	427	✓			
36.4	11.00	0	0	-23	0	0	16.3	5.0	124			*188	1296	99	683	28	193	46	317	15	103	2480	1.600	56	386	✓			
36.4	11.00	0	0	-23	0	0	17.0	4.1	111			*128	882	93	641	26	179	48	331	25	172	2780	1.793	50	345	✓			
31.2	9.51	0	0	-25	0	0	12.4	4.9	72			*159	1096	63	434	26	179	33	227	12	83	2240	1.445	48	331	✓			
31.0	9.45	0	0	-26	0	0	9.3	2.8	62			*90	620	47	324	26	179	33	227	13	90	1920	1.239	41	283	✓			
31.0	9.45	0	0	-27	0	0	8.3	3.5	60			92	634	32	221	20	138	26	179	12	83	2160	1.394	37	255	✓			
36.0	11.00	0	0	-27	0	0	14.1	4.6	92			*97	669	31	214	15	103	37	255	15	103	2370	1.529	50	345	✓			
30.4	9.27	0	0	-30	0	0	7.2	2.9	54			*63	434	*24	165	17	117	16	110	11	76	1280	.826	50	345	✓			
30.2	9.20	0	0	-35	0	0	5.3	2.4	29			*42	289	19	131	8	55	15	103	7	48	3390	2.187	14	97	✓			
29.8	9.08	0	0	-39	0	0	4.1	1.9	29			*30	207	15	103	8	55	11	76	5	34	2460	1.587	15	103	✓			
31.8	9.69	30	9.1	-11	0	0	36.8	7.1	132			85	586	156	1076	90	620	*113	779	*8	55	6530	4.213	50	345	✓	✓		
31.6	9.63	30	9.1	-14	0	0	32.0	7.1	125			194	1338	104	717	106	731	105	724	12	83	4720	3.045	60	414	✓	✓		
31.2	9.51	30	9.1	-21	0	0	17.5	6.9	75			188	1296	84	579	15	103	48	331			3680	2.374	41	283	✓	✓		
30.9	9.42	30	9.1	-23	0	0	11.7	5.1	84			113	779	37	255	10	69	22	157	6	41	2320	1.497	44	303	✓			
30.4	9.27	30	9.1	-28	0	0	6.9	3.6	47			*57	393	14	97	4	28	*10	69	1	7	1570	1.013	39	269	✓			
29.9	9.11	30	9.1	-35	0	0	3.7	3.3	23			*28	193	8	55	1	7	*6	41	0	0	1200	.774	32	221	✓			
30.0	9.14	30	9.1	-38	0	0	3.4	3.0	28			*21	145	5	34	0	0	3	21	0	0	1170	.755	32	221	✓			
31.2	9.51	50	15	-12	0	0	37.8	7.5	162			113	779	148	1020	64	441	*93	641	0	0	6110	3.942	50	345	✓	✓		
31.0	9.45	50	15	-15	0	0	27.6	7.0	182			180	1241	83	572	84	579	84	579	2	14	4100	2.645	46	317	✓	✓		
30.4	9.27	49	15	-20	0	0	16.6	5.7	121			185	1276	88	607	12	83	43	296	0	0	2900	1.871	50	345	✓	✓		
30.0	9.14	50	15	-28	0	0	8.8	4.5	61			*58	400	17	117	1	7	7	48	0	0	1600	1.032	50	345	✓			
29.6	9.02	49	15	-30	0	0	6.3	4.2	37			*41	283	6	41	1	7	7	48	0	0	1350	.871	41	283	✓			
29.4	8.96	49	15	-33	0	0	4.2	4.3	28			27	186	5	34	0	0	8	55	0	0	1250	.806	33	228	✓			
29.2	8.90	49	15	-36	0	0	2.7, -2.7	4.6	19, -19			*18	124	0	0	0	0	0	0	0	0	1020	.658	29	200	✓			
32.0	9.75	30	9.1	-16	180	0	23.4	3.6	151			*208	1434	*92	634	121	834	112	772	45	310	4640	2.994	42	290	✓			
31.6	9.63	30	9.1	-21	180	0	15.4	3.9	107			*184	1268	*134	924	46	317	75	517	28	193	3600	2.323	37	255	✓			
31.2	9.51	30	9.1	-25	180	0	12.9	5.7	89			136	938	86	593	42	290	53	365	18	124	2420	1.561	46	317	✓			
30.8	9.39	30	9.1	-30	180	0	9.1	3.0	58			*88	607	*48	331	29	200	39	269	20	138	1540	.994	52	359	✓			
30.6	9.33	30	9.1	-33	180	0	8.5	1.9	51			*80	552	46	317	29	200	35	241	15	103	1470	.948	43	296	✓			
30.2	9.20	30	9.1	-39	180	0	6.4	1.6	37			*53	365	32	221	22	152	24	165	14	97	1360	.877	32	221	✓			
30.2	9.20	30	9.1	-41	180	0	6.1	1.5	37			*42	290	*27	186	20	138	23	159	13	90	1180	.761	35	241	✓			
31.9	9.72	50	15	-10	180	0	33.7	3.9	84, -98			27	186	*100	689	121	834	*156	1076	91	627	5280	3.406	54	372	✓			
30.0	9.14	50	15	-18	180	0	18.8	4.4	97			*105	724	*120	827	136	938	136	938	44	303	3420	2.206	48	331	✓			
30.0	9.14	50	15	-22	180	0						164	1131	108	745	62	427	87	600	10	69					✓			
30.0	9.14	50	15	-30	180	0	8.2	2.0	56			*100	689	59	407	39	269	50	345	20	138	3570	2.303	22	152	✓			
30.2	9.20	50	15	-30	180	0	9.4	2.1	51			92	634	48	331	38	262	48	331	17	117	3380	2.181	24	165	✓			
29.5	8.99	50	15	-39	180	0	7.6	1.7	42			72	496	43	296	30	207	35	241	18	124	4530	2.923	14	97	✓			
29.8	9.08	50	15	-40	180	0	6.7	1.7	42			66	455	39	269	28	193	33	228	18	124	3840	2.477	16	110	✓			
31.1	9.48	0	0	-24	0	0	11.7	3.1	84			298.1	4350	*109	752	65	448	25	172	35	241	13	90	2270	1.465	49	338	✓	
31.2	9.51	0	0	-25	0	0	11.5	3.8	74			*50	345	63	434	26	179	38	262	20	138	2220	1.432	50	345	✓			
31.0	9.45	0	0	-26	0	0	9.6	4.1	62			*76	524	54	372	22	152	30	207	7	48	2110	1.361	47	324	✓			
31.2	9.51	0	0	-25	0	0	10.7	4.4	61			329.2	4804	*111	765	59	408	25	172	34	234	13	90	2180	1.406	53	365	✓	
31.2	9.51	0	0	-25	0	0	9.8	4.3	60			*93	641	62	427	26	179	37	255	16	110	2180	1.406	52	359	✓			
36.2	11.00	0	0	-25	0	0	13.0	5.2	93			*129	889	75	517	31	214	48	331	28	193	2420	1.561	61	421	✓			
31.0	9.45	0	0	-27	0	0	8.5	3.1	56			*93	641	52	359	22	152	28	193	13	90	2350	1.516	38	262	✓			

*Integrated the pressure distribution.

TABLE V.- ADDITIONAL MAXIMUM ACCELERATION DATA FOR WATER LANDINGS

[All values are full scale]

Vertical velocity		Horizontal velocity		Landing attitude			Normal acceleration at c.g., g units	Longitudinal acceleration at c.g., g units	Angular acceleration, rad/sec ²	Transverse acceleration, g units	Stability	
ft/sec	m/sec	ft/sec	m/sec	Pitch, deg	Roll, deg	Yaw, deg					Stable	Turnover
30	9.1	0	0	-1	0	0	50				✓	
23	7.0			1			30				✓	
21 to 23	6.4 to 7.0			1			29	-2.5, 3.8	-56		✓	
				4			27	-3.4, 2.0	-95, 45		✓	
				10			21	-4.3, 2.9	-129, 28		✓	
				12			18	-4.2	-112		✓	
				20			7	-3.8	-90		✓	
				29			3	-1.5	-45		✓	
				-4			27	-0.5, 3.3	72, -56		✓	
				-9			24	3.5	135, -39		✓	
				-14			16	3.3	113		✓	
				-19			13	2.8	78		✓	
				-25			8	2.3	62		✓	
		10	3.0	-1			30	-0.4, 2.9	-61, 55		✓	
				-2			29	-1.3, 3.3	-78		✓	
				-7			30	3.8	78, -55		✓	
				-12			25	4.0	122, -33		✓	
				-30			4.5	1.8	39		✓	
		20	6.1	0			30	-1.5, 3.0	-85, 68			✓
				-5			30	4.0	61, -55			✓
				-10			27	5.3	144, -44			✓
				-22			8	3.0	61			✓
		30	9.1	0			31	2.9	-34, 62		✓	
				0			29	-0.6, 4.2	-50, 67			✓
				6			27	-2.1, 3.1	-100, 67			✓
				10			19	-3.7, 2.1	-72, 33			✓
				16			11	-4.4	-101			✓
				22			7	-3.2	-106		✓	
				-5			30	4.5	89, -44			✓
				-10			26	4.8	122, -44			✓
				-15			16	5.0	90			✓
				-18			12	3.5	89			✓
				-19			12	3.8	90			✓
				-29			4	2.0	33		✓	
		40	12.0	1			28	-1.5, 3.5	-61, 89			✓
				-4			27	5.0	66, -66			✓
				-10			25	7.0	133			✓
				-20			9.8	2.5	67			✓
		50	15.0	3			27	-1.5, 3.8	-55, 89		✓	
				-2			26	-1.3, 4.3	-55, 61			✓
				-11			26	5.0	127			✓
				-28			10.2	3.8	78			✓
		10	3.0	-5		90	27	3.2	45, -50	0.5	✓	
		20	6.1	-1			26	-0.9, 2.5	45, -45	0.7	✓	
		30	9.1	-2			29	-1.5, 3.4	-73	0.7, 1.8	✓	
		40	12.0	3			27	-2.5, 3.0	44, -50	-2.6, 2.0	✓	
		50	15.0	5			26	-1.9, 2.0	-45	-2.4, 2.6	✓	
		10	3.0	-2		180	29	1.8, -2.1	45, -67		✓	
		20	6.1	-6			28	2.5	95, -67		✓	
		30	9.1	1			28	-2.8, 2.0	-130		✓	
				8			22	-5.4, 2.6	-140		✓	
				14			13	-4.5	-123		✓	
				19			7	-4.0	112		✓	
				24			8	2.4	56		✓	
				-2			29	-3.5	17, -146		✓	
				-6			29	2.6	107, -57		✓	
				-12			19	4.0	101, -56		✓	
				-15			15	3.4	101		✓	
				-16			15	3.8	101		✓	
		40	12.0	-6			28	1.6, -0.9	78, -84		✓	
		50	15.0	-3			27	0.5, -1.8	39, -112			✓

TABLE VI.- MAXIMUM ACCELERATION DATA FOR LANDINGS ON SAND

[All values are full scale]

Vertical velocity		Horizontal velocity		Landing attitude			Normal acceleration, g units	Longitudinal acceleration, g units	Angular acceleration, rad/sec ²	Remarks
ft/sec	m/sec	ft/sec	m/sec	Pitch, deg	Roll, deg	Yaw, deg				
23	7.0	0	0	0	0	0	49.3	6.3	-57	Heat-shield failure
23	7.0	0	0	-5	0	0	47.3	7.6	36, -57	Heat-shield failure
23	7.0	0	0	-10	0	0	28	13.2	130	

TABLE VII.- MAXIMUM ACCELERATION DATA FOR LANDINGS

ON A HARD CLAY-GRAVEL LANDING SURFACE

[All values are full scale]

Vertical velocity		Horizontal velocity		Landing attitude			Normal acceleration, g units	Longitudinal acceleration, g units	Angular acceleration, rad/sec ²	Stability		Remarks
ft/sec	m/sec	ft/sec	m/sec	Pitch, deg	Roll, deg	Yaw, deg				Stable	Turnover	
23	7.0	30	9.1	0	0	0	40	10.2	-128		✓	Heat-shield failure
23	7.0	30	9.1	-10	0	0	42.5	25.5	241		✓	Heat-shield failure
23	7.0	30	9.1	-20	0	0	42.5	34.3	362		✓	Heat-shield failure
23	7.0	30	9.1	-30	0	0	39	21.3	640		✓	Heat-shield failure

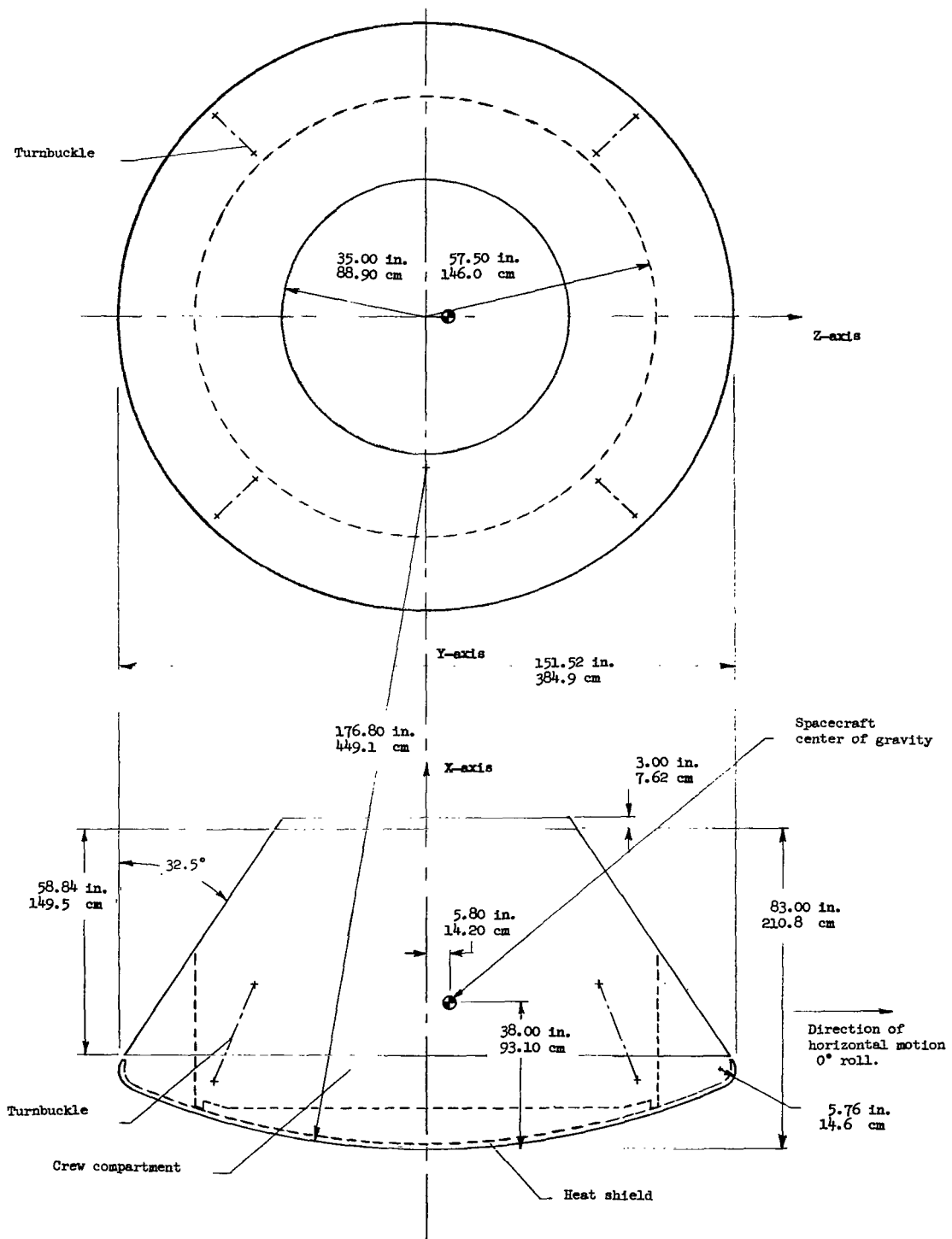
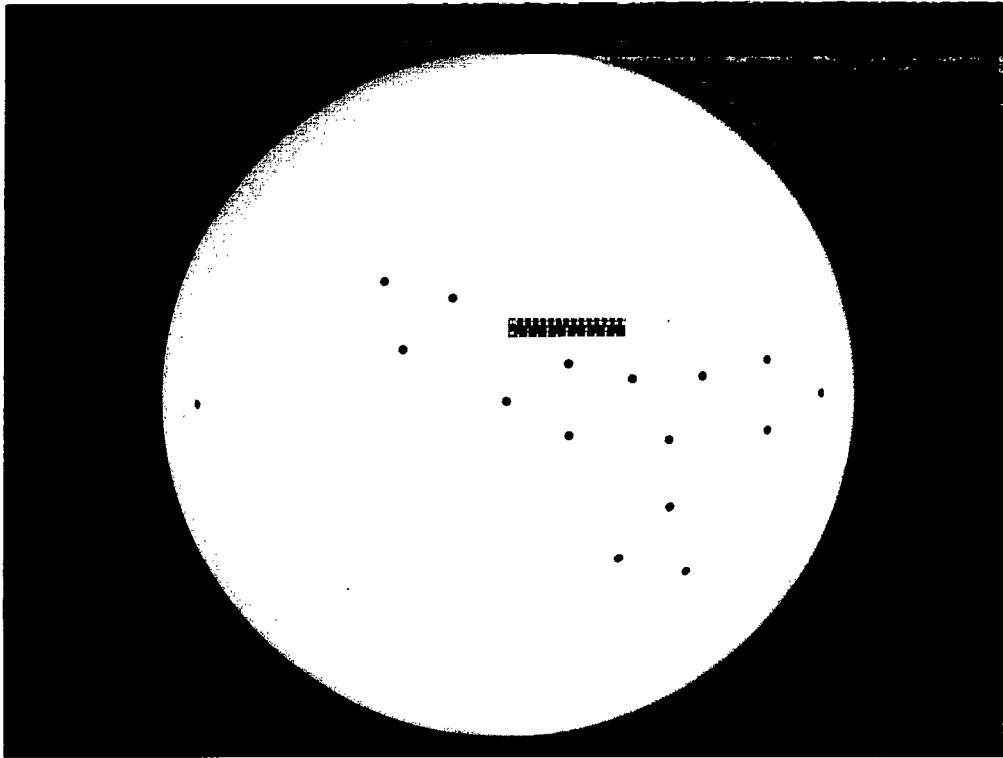
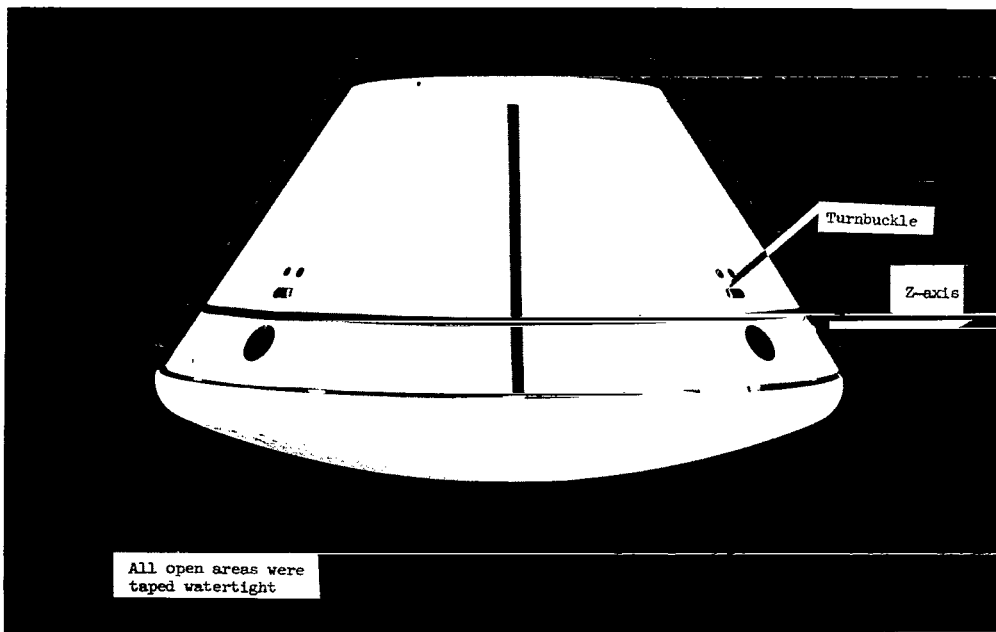


Figure 1.- Dimensions of the prototype Apollo spacecraft from which model was scaled. All values are full scale.



Bottom view

L-65-8012



Side view

Figure 2.- Photograph of 1/4-scale model.

L-63-6193

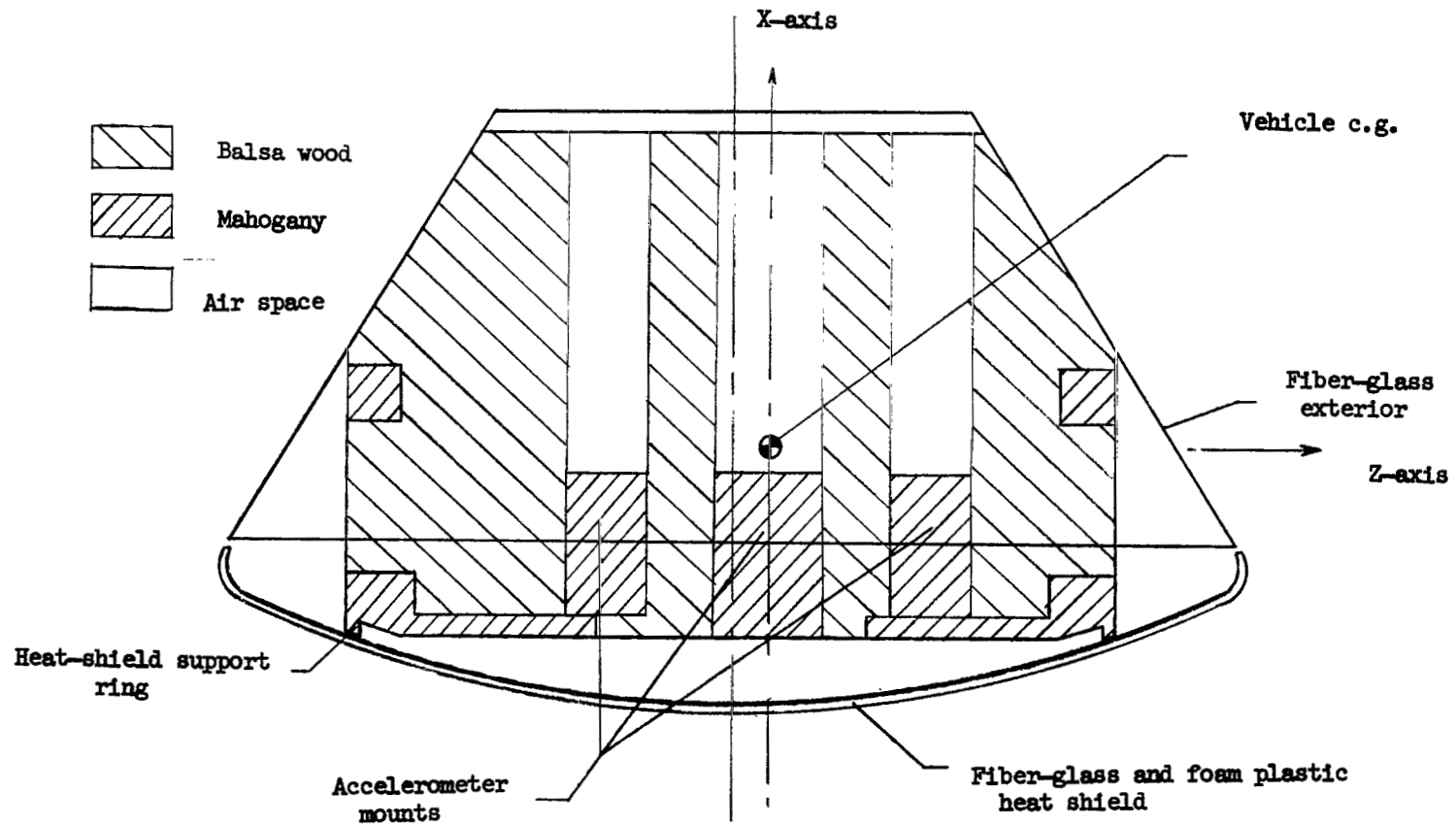


Figure 3.- Cross section of model showing construction details.

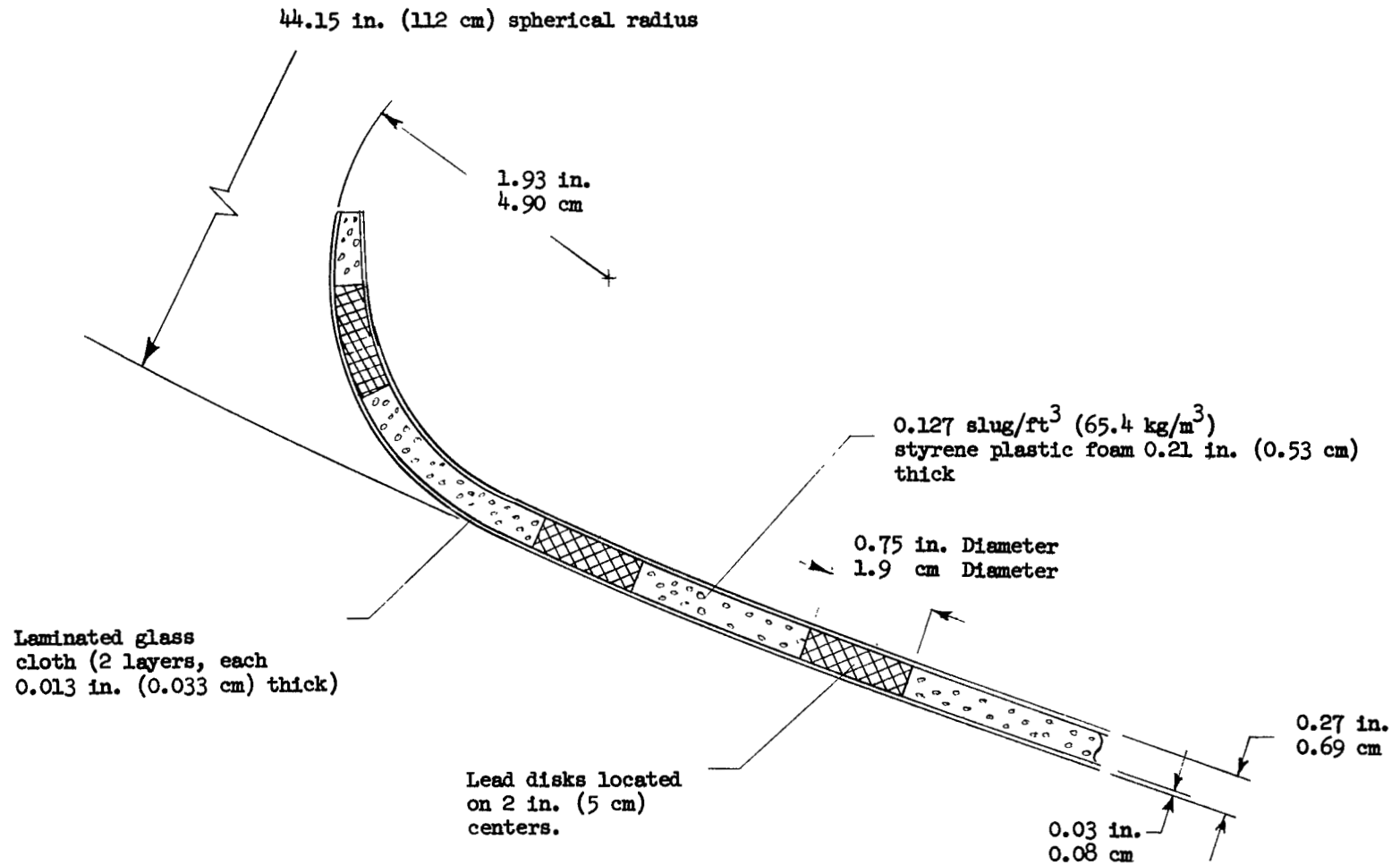


Figure 4.- Heat-shield construction details. All values are model dimensions.

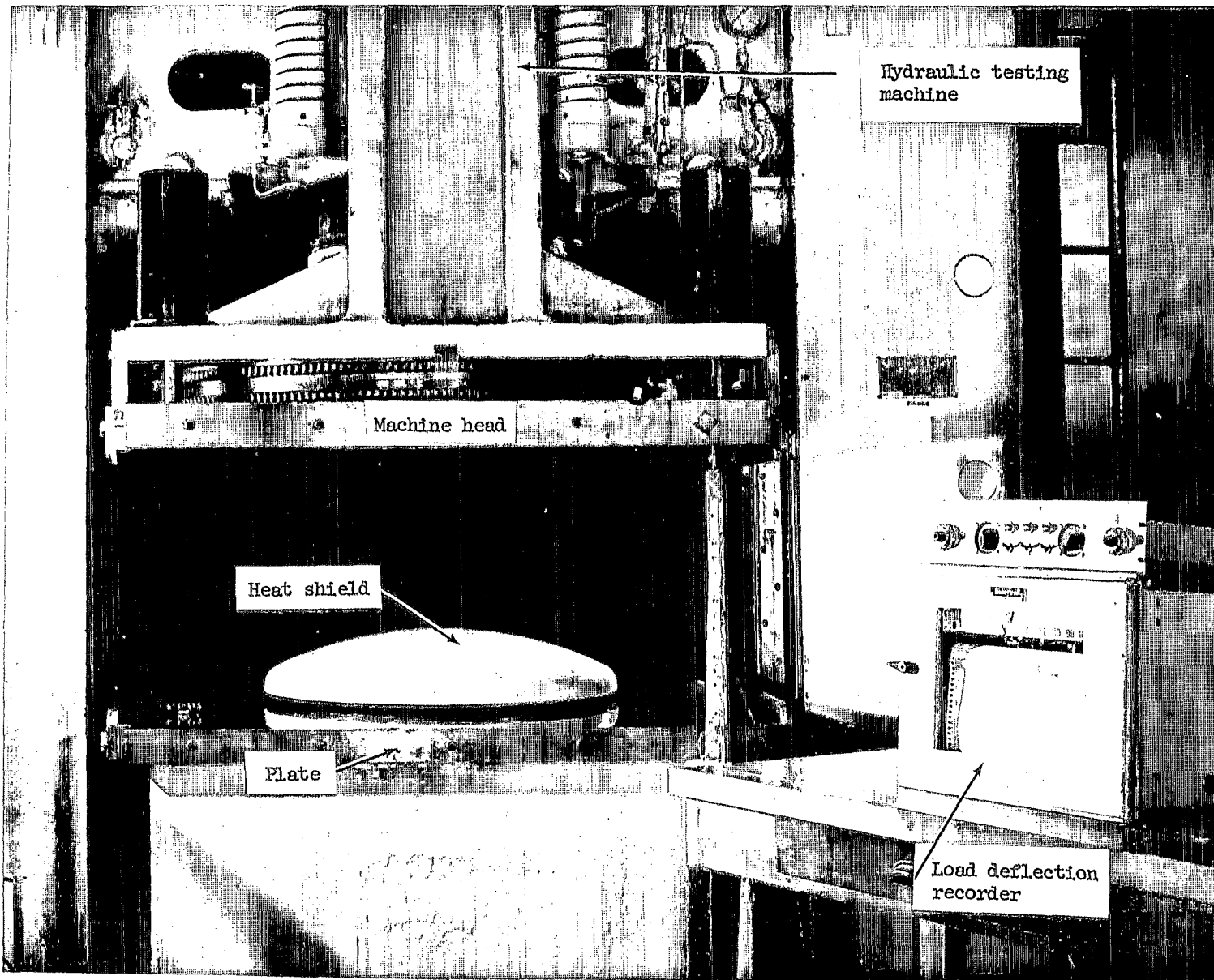


Figure 5.- Setup used to determine heat-shield stiffness.

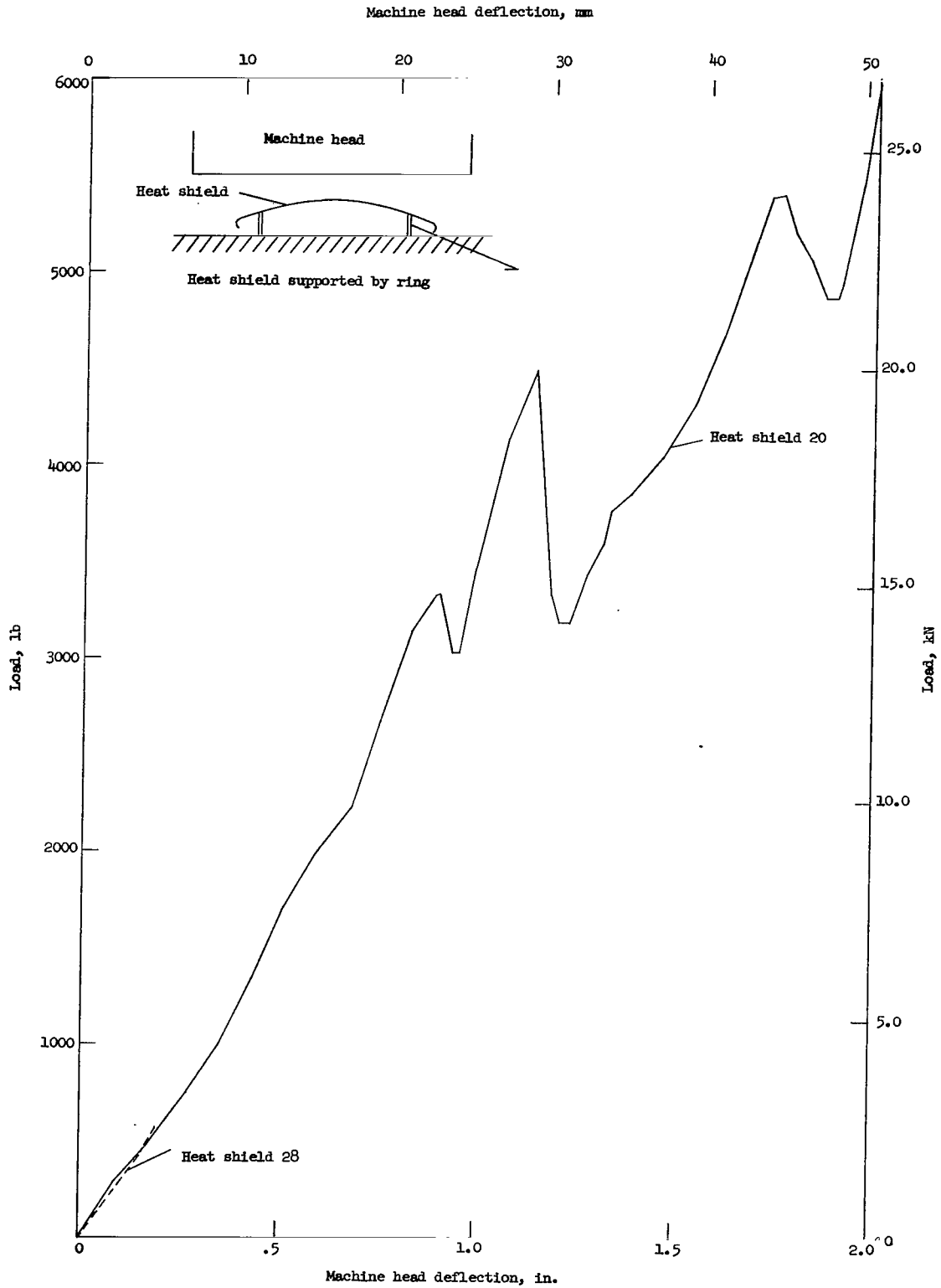


Figure 6.- Force deflection characteristics for model heat shield. All values are model scale.

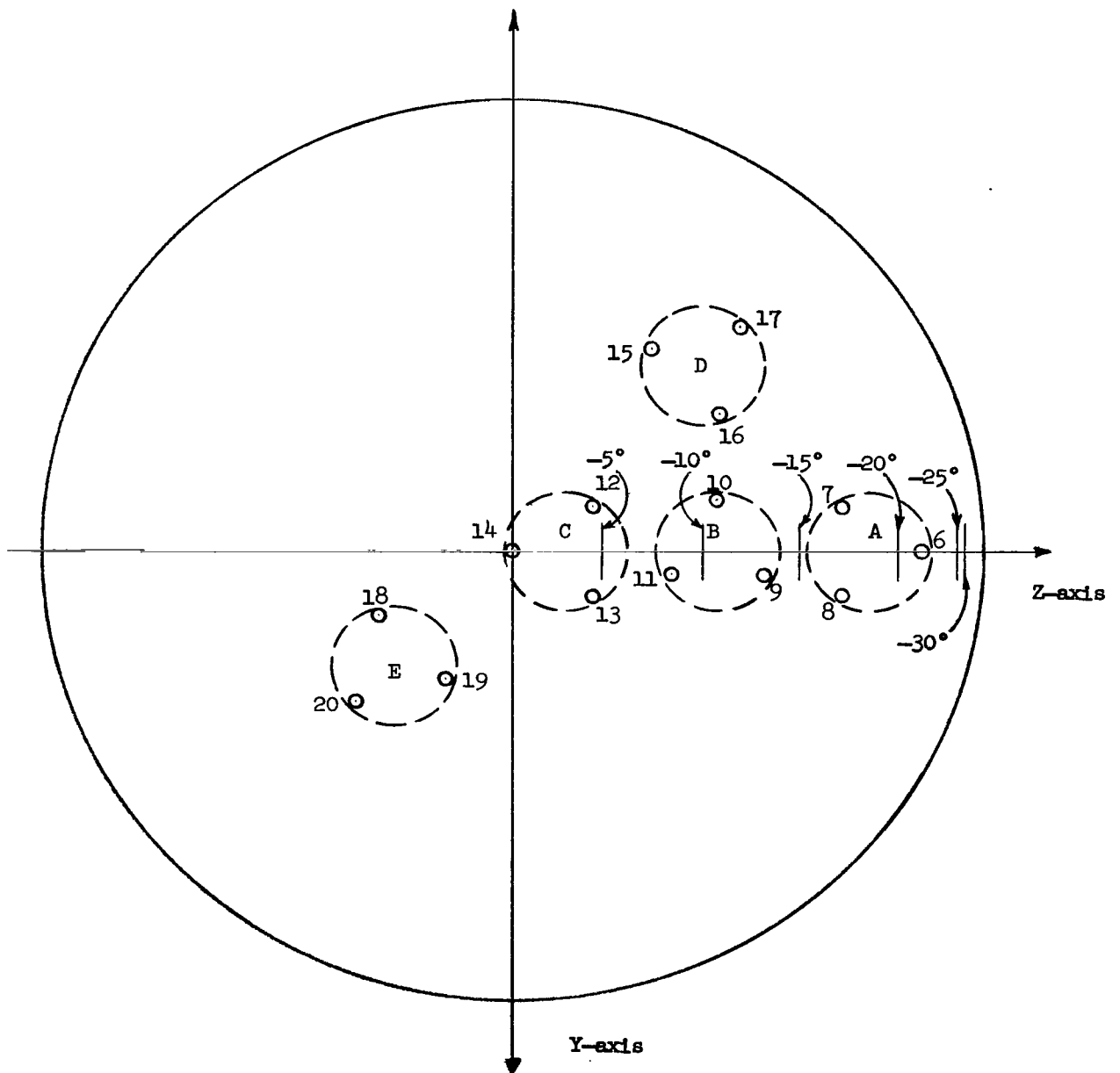


Figure 7.- Sketch showing locations of pressure transducers and panel areas on heat shield. (Numbers 6 to 21 are arbitrarily assigned to the pressure transducers. Letters A, B, C, D, and E denote arbitrary panel areas. Angles show initial points of water contact on the heat shield for various pitch-landing attitudes.)

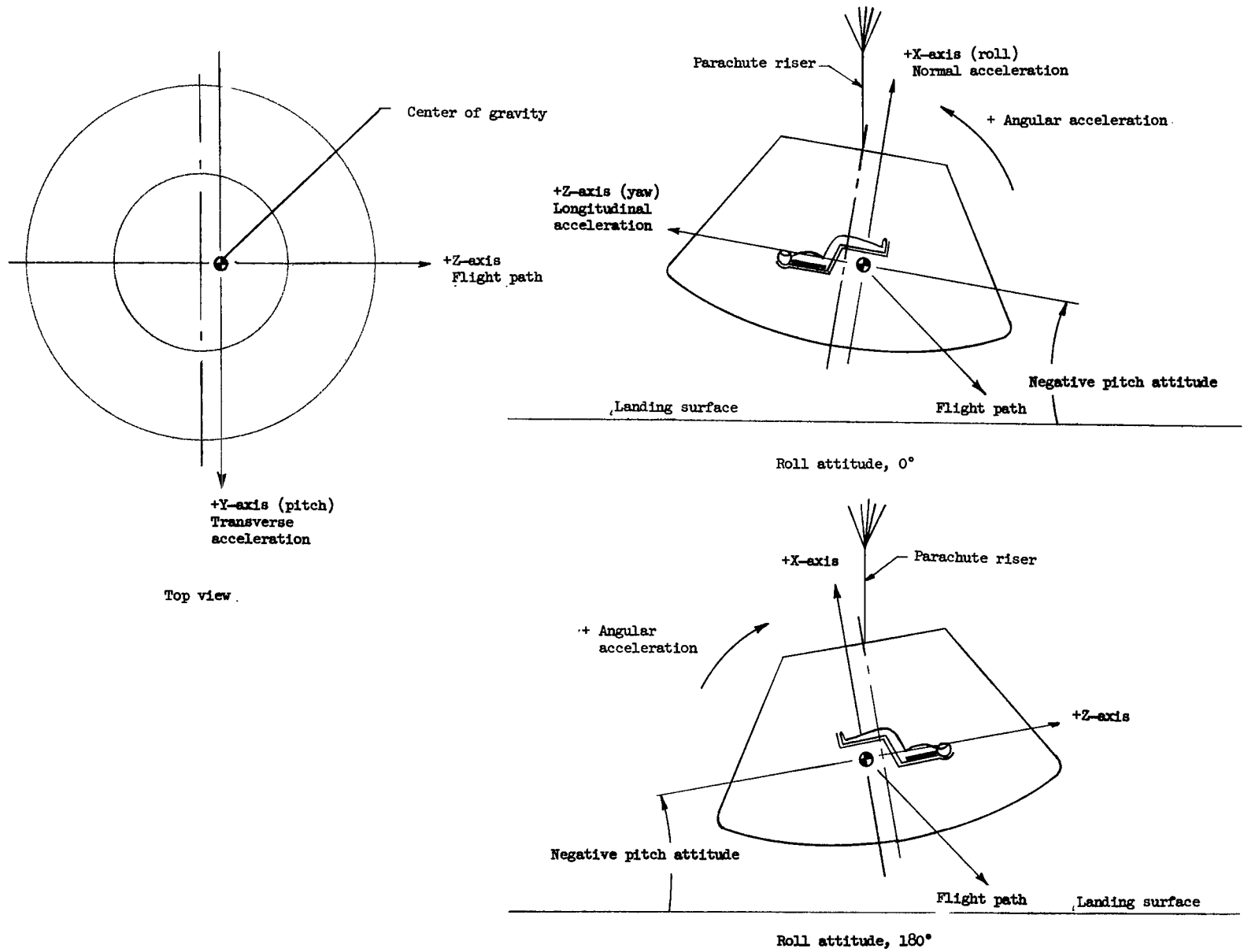


Figure 8.- Sketches identifying acceleration axes, attitudes, force directions, and flight path.

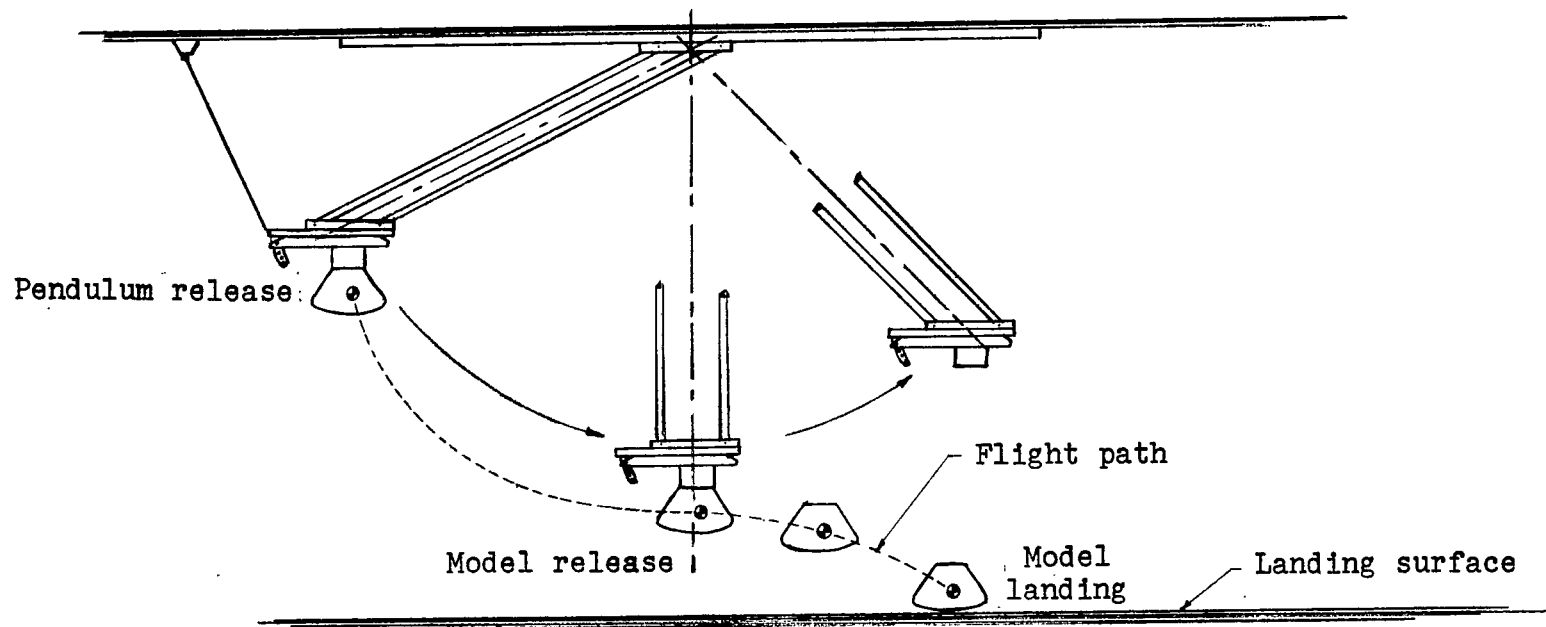


Figure 9.- Sketch showing pendulum operation during typical model launch and landing.

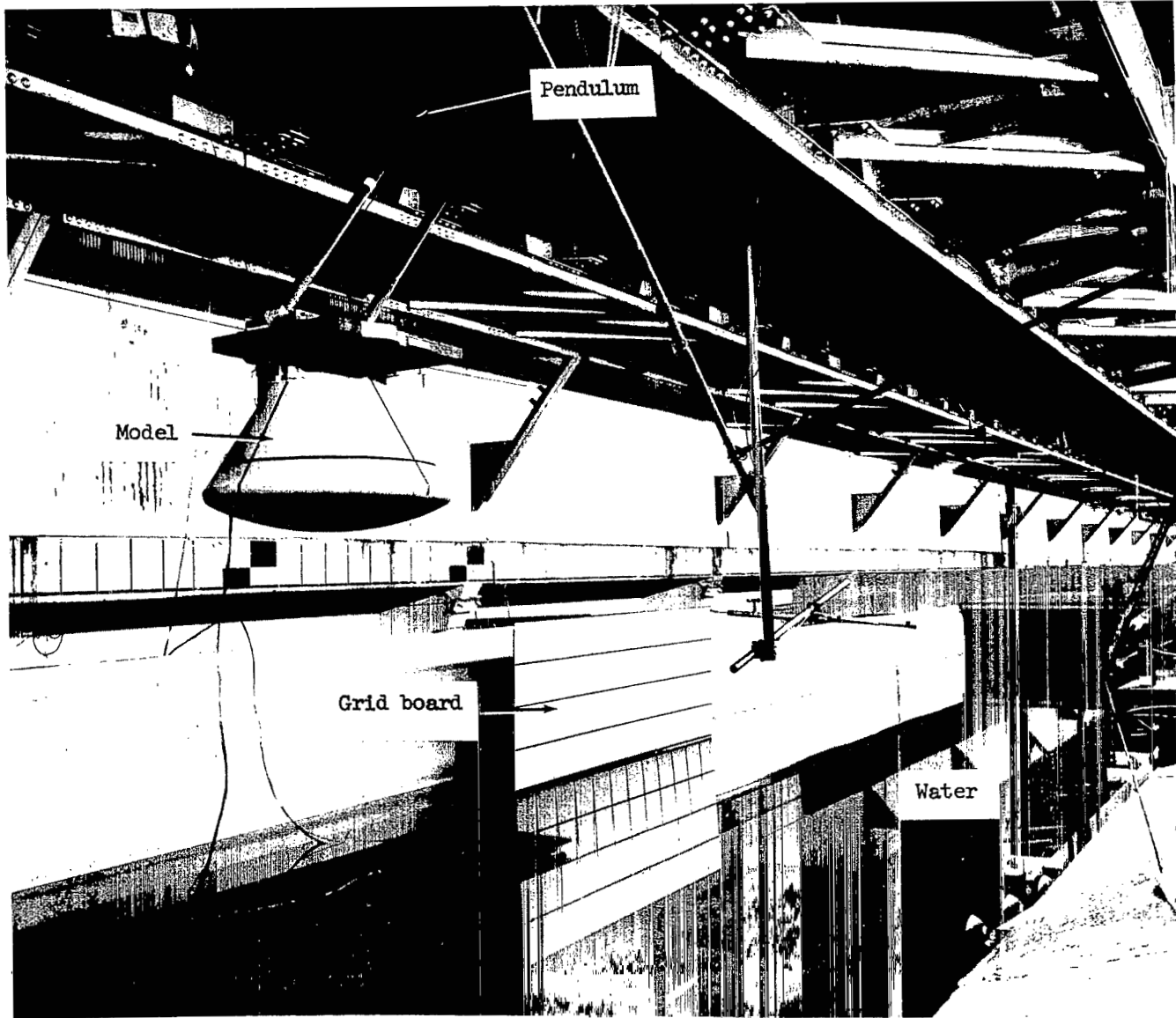
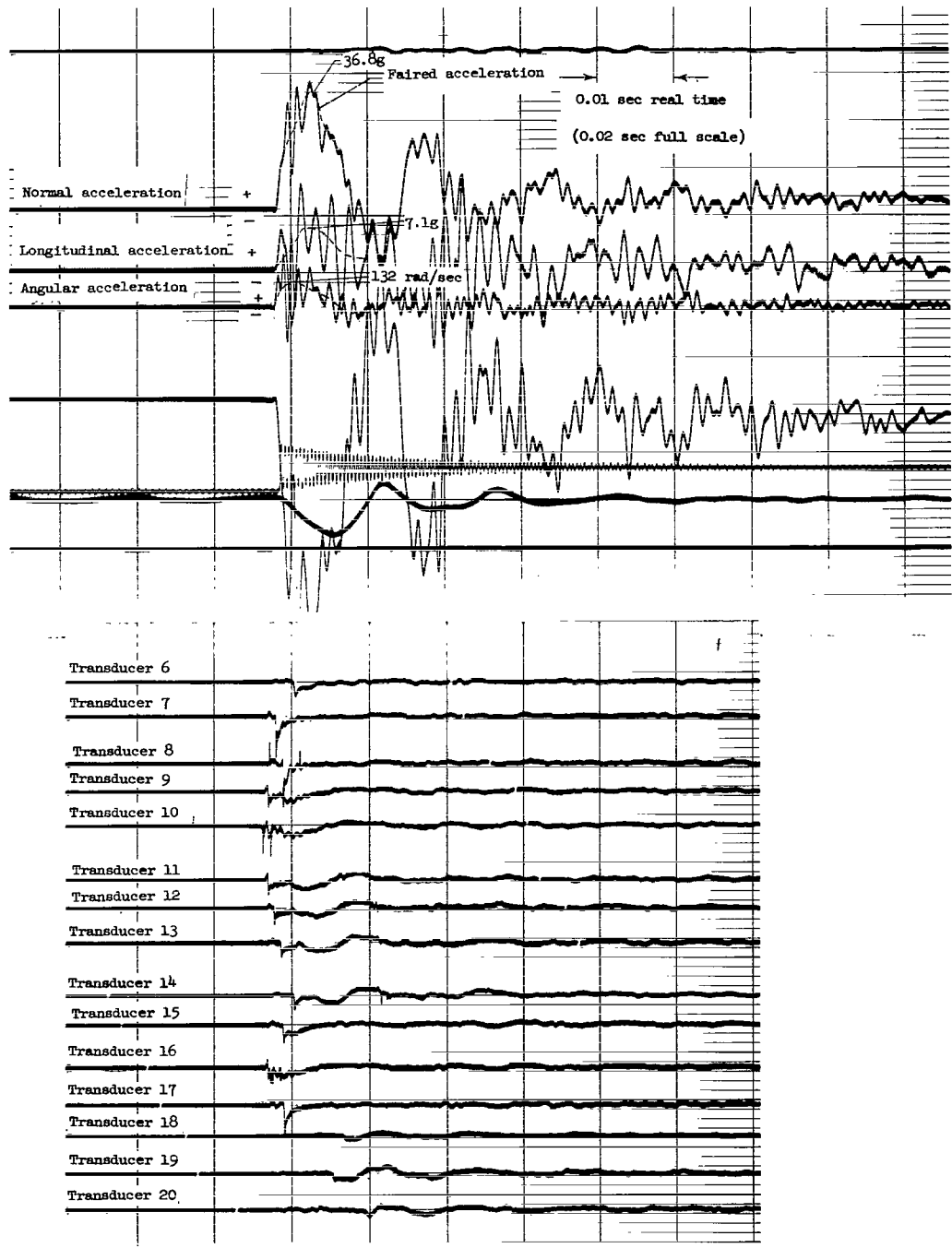
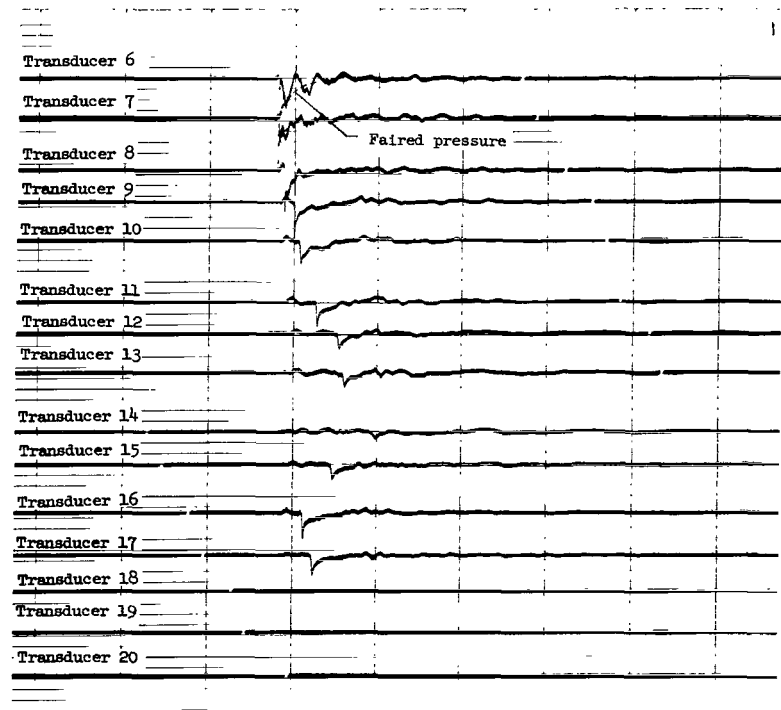
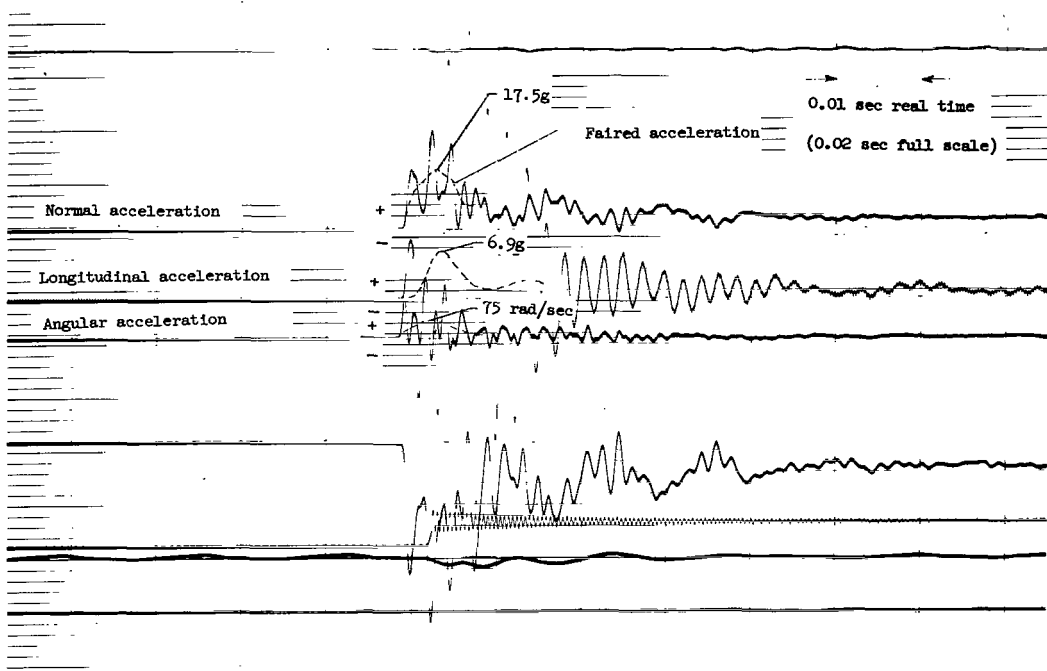


Figure 10.- Test area setup showing model on carriage in pulled-back position.

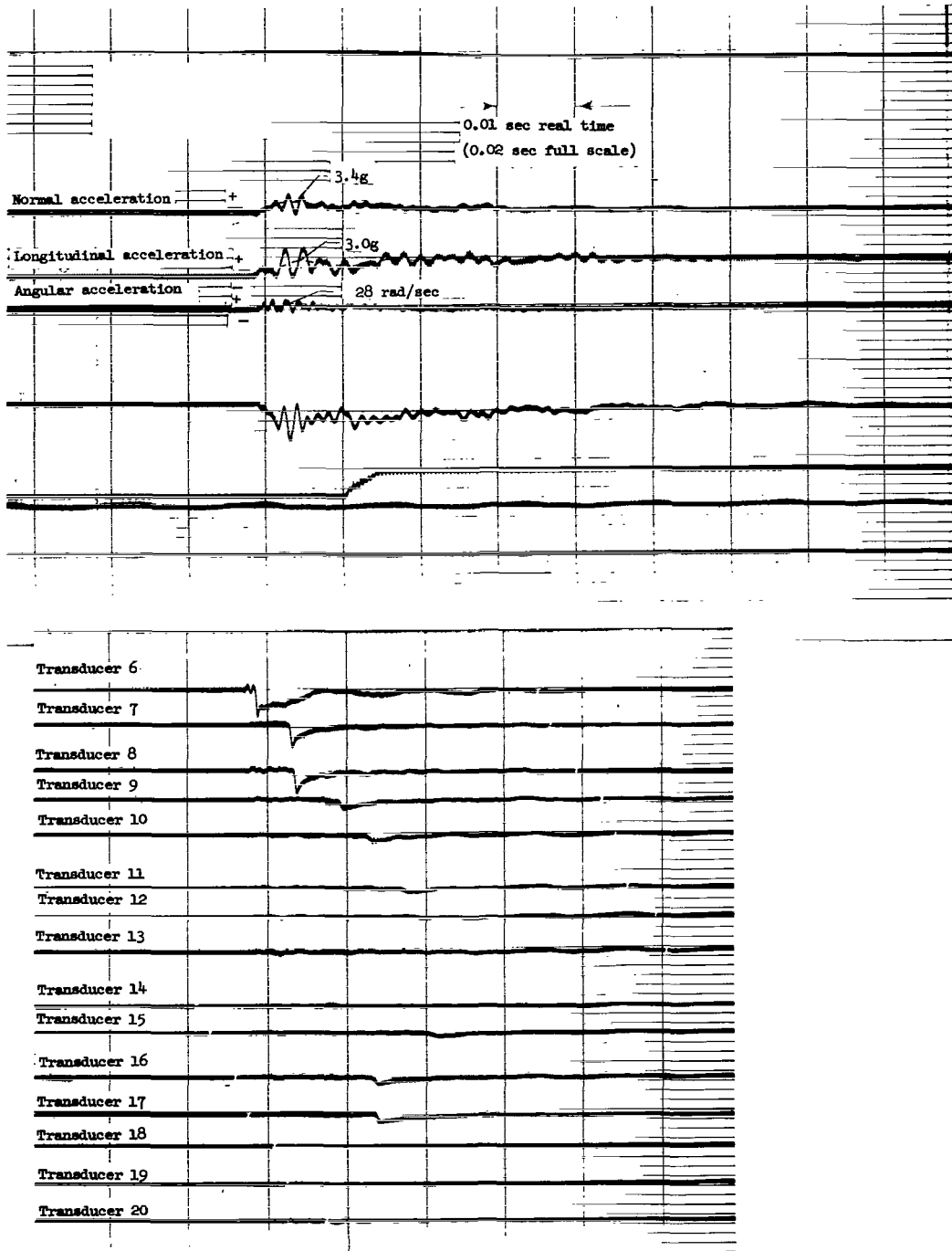


(a) Pitch attitude, -11° .

Figure 11.- Typical oscillograph records of accelerations and pressures for landings on water. Vertical velocity, 30 ft/sec (9.1 m/s); horizontal velocity, 30 ft/sec (9.1 m/s); roll, 0° ; yaw, 0° . All values are full scale unless otherwise indicated.

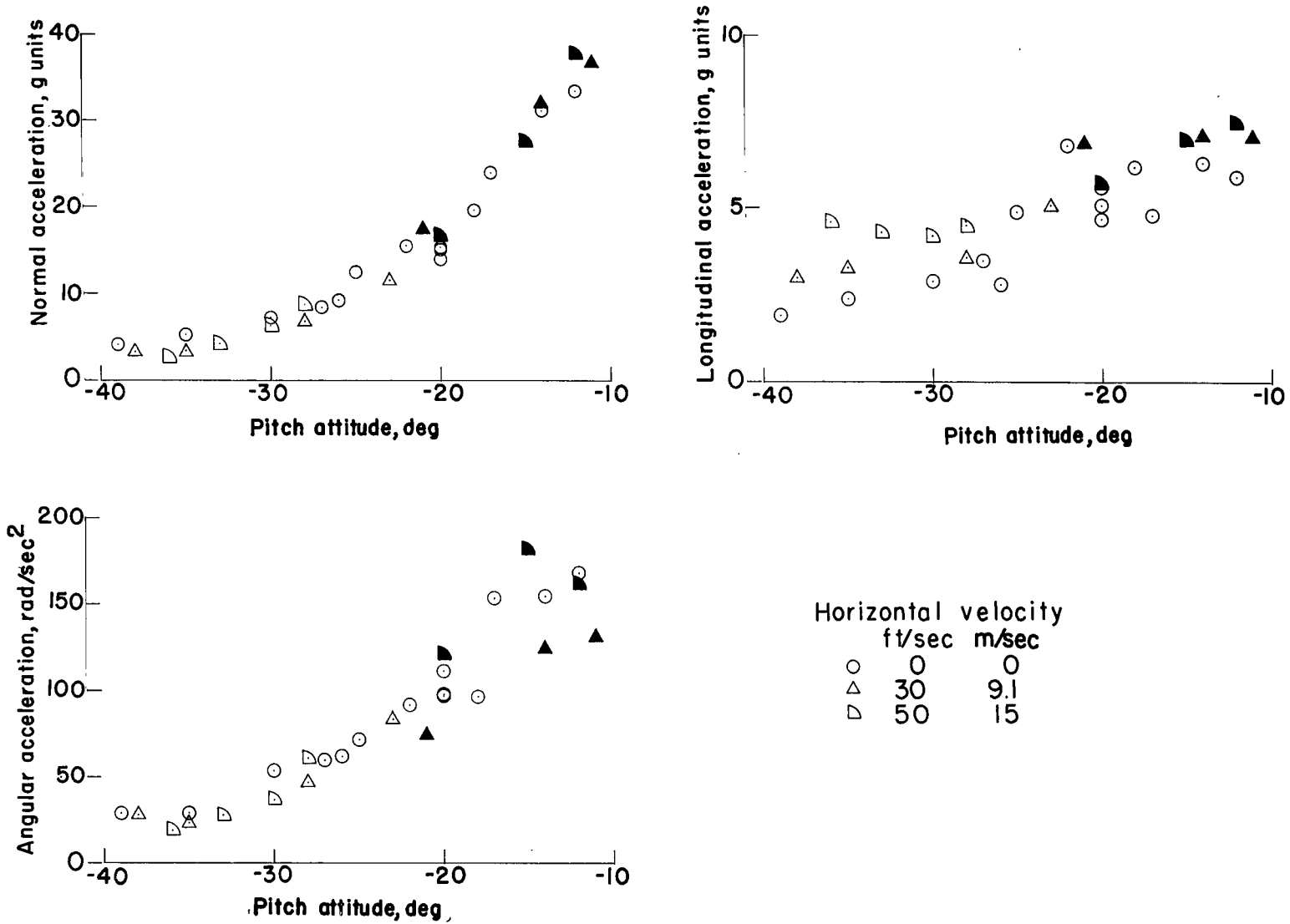


(b) Pitch attitude, -21° .
Figure 11.- Continued.



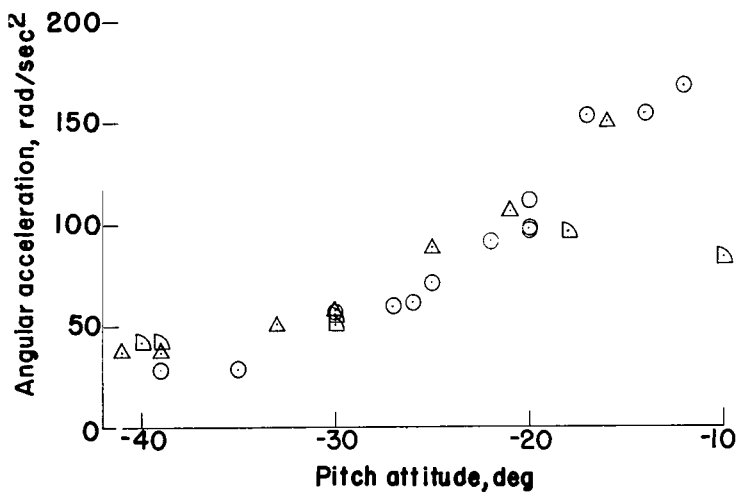
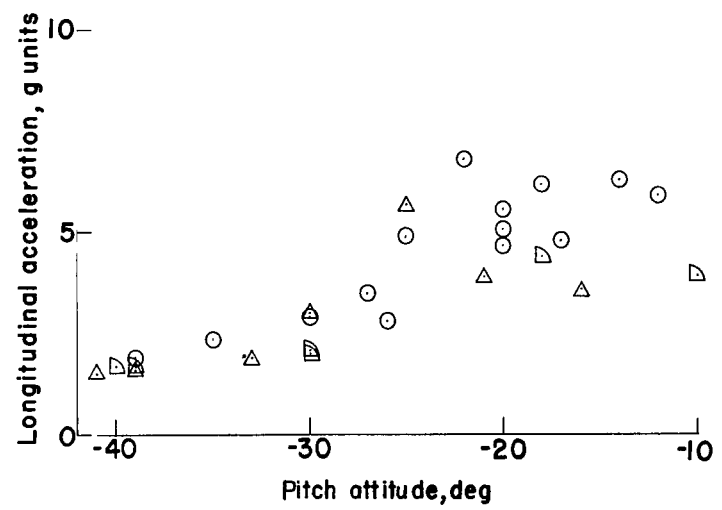
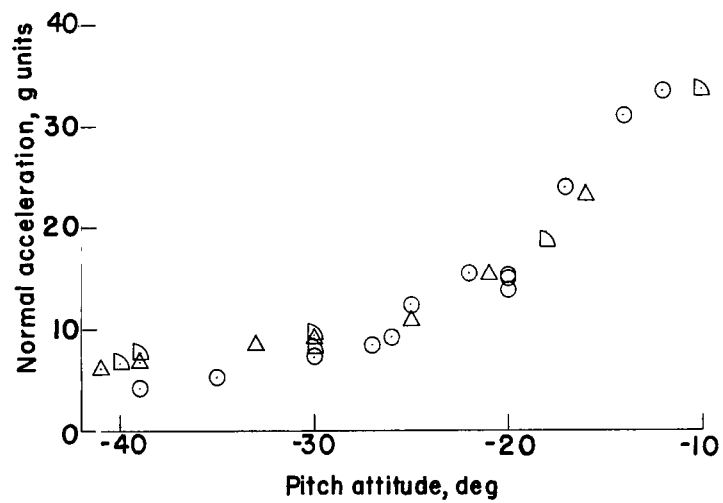
(c) Pitch attitude, -38° .

Figure 11.- Concluded.



(a) Roll, 0°.

Figure 12.- Maximum acceleration data for water impact pressure investigation. Vertical velocity, 29.2 to 32.4 ft/sec (8.90 to 9.88 m/sec); yaw, 0°. All values are full scale. (Shaded data points indicate turnover.)



Horizontal velocity

	ft/sec	m/sec
○	0	0
△	30	9.1
▽	50	15

(b) Roll, 180°.

Figure 12.- Concluded.

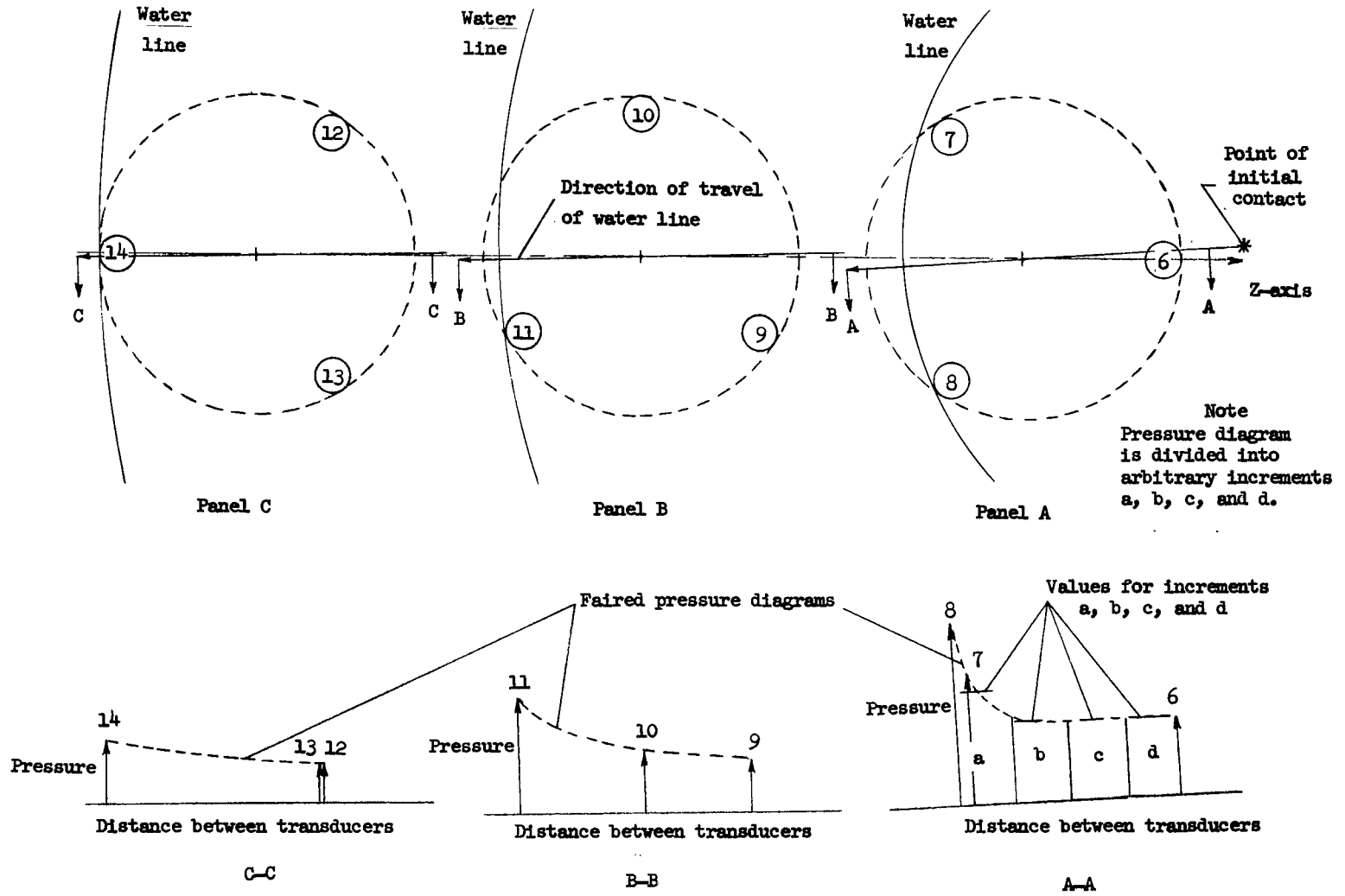


Figure 13.- Sketches of typical pressure panels to show method of obtaining mean pressures.

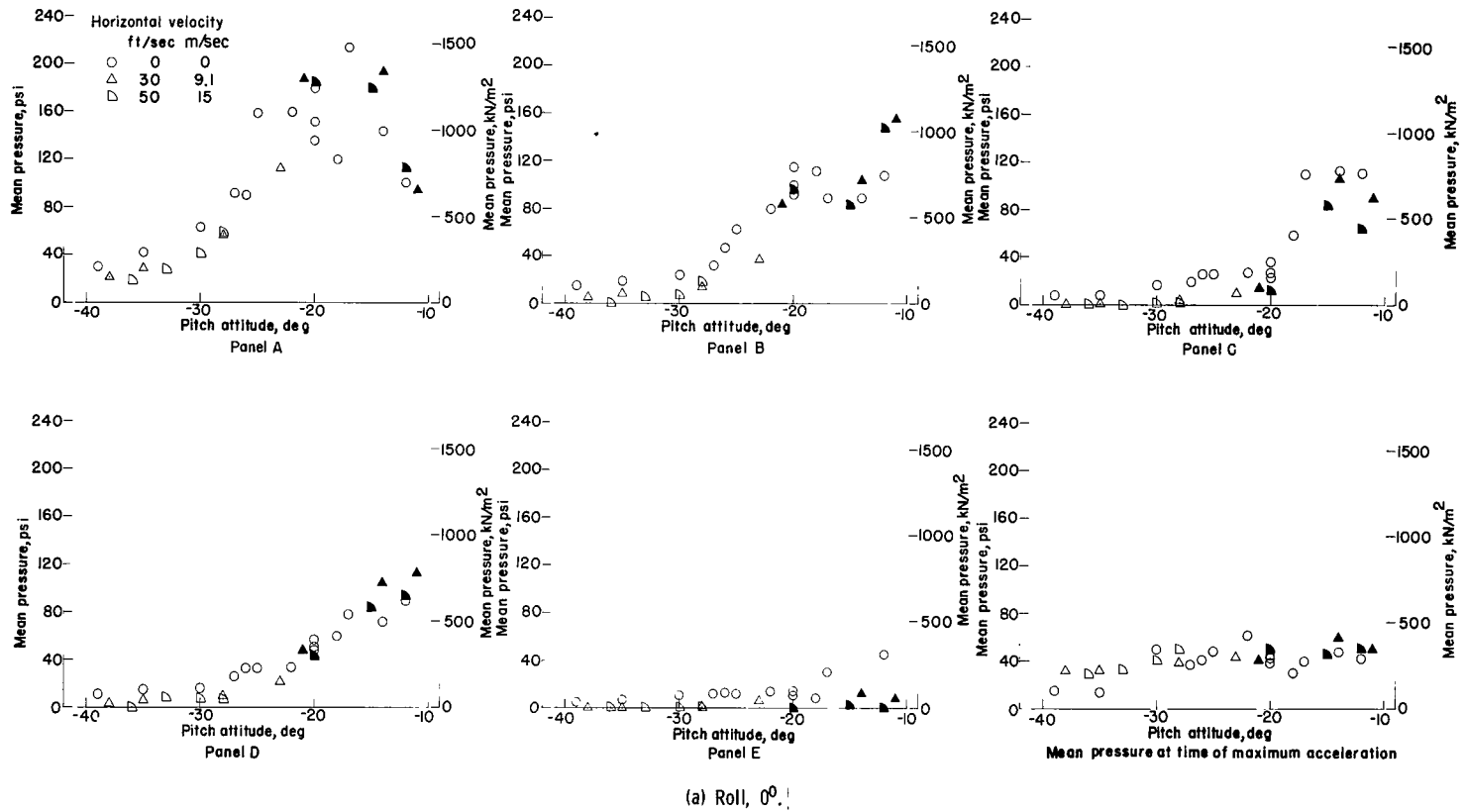
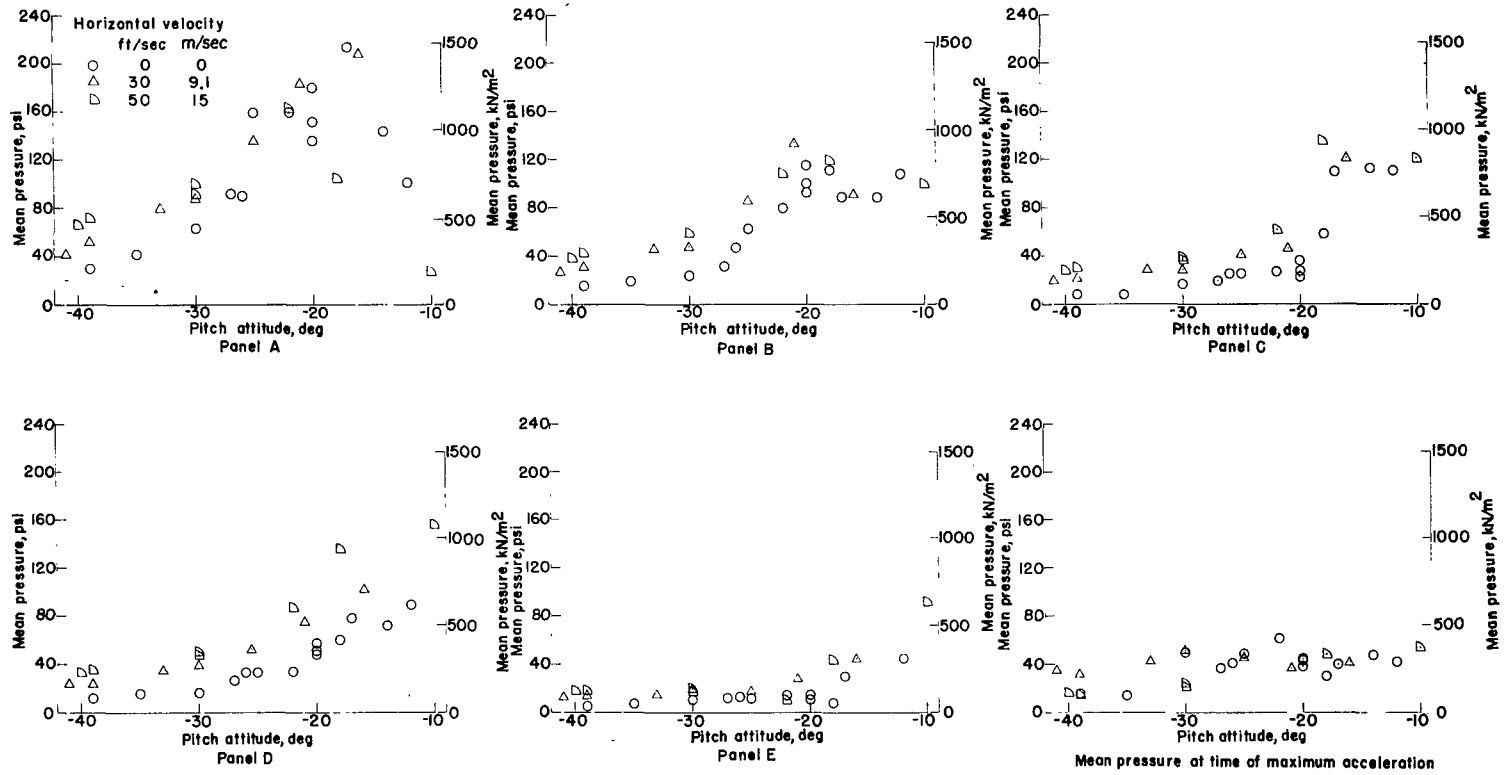
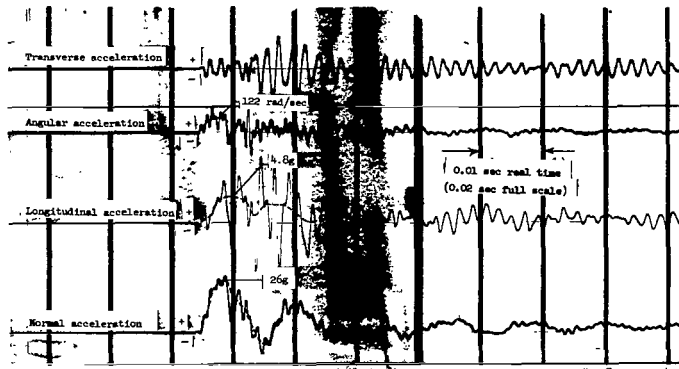


Figure 14.- Mean pressures occurring on each panel for each test in water impact pressure investigation. Vertical velocity, 29.2 to 32.4 ft/sec (8.90 to 9.88 m/sec); yaw, 0°. Also included is mean pressure over the wetted area at time of maximum acceleration. All values are full scale. (Shaded data points indicate turnover.)

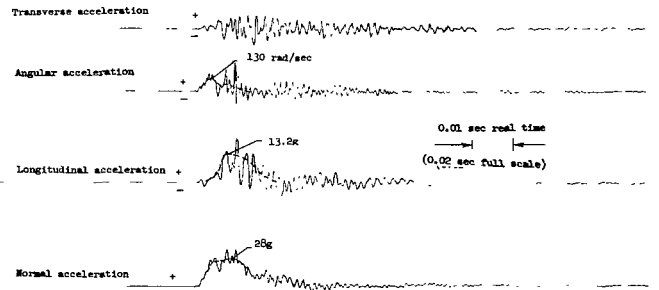


(b) Roll, 180°.

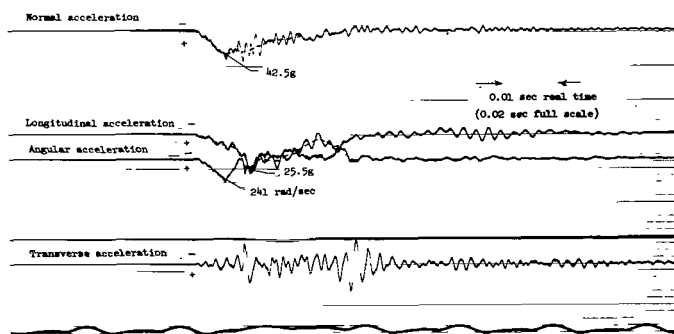
Figure 14.- Concluded.



(a) Landing on calm water; horizontal velocity, 30 ft/sec (9.1 m/sec).

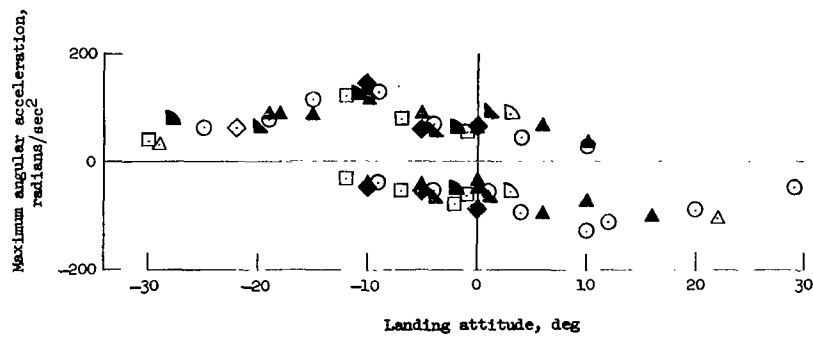
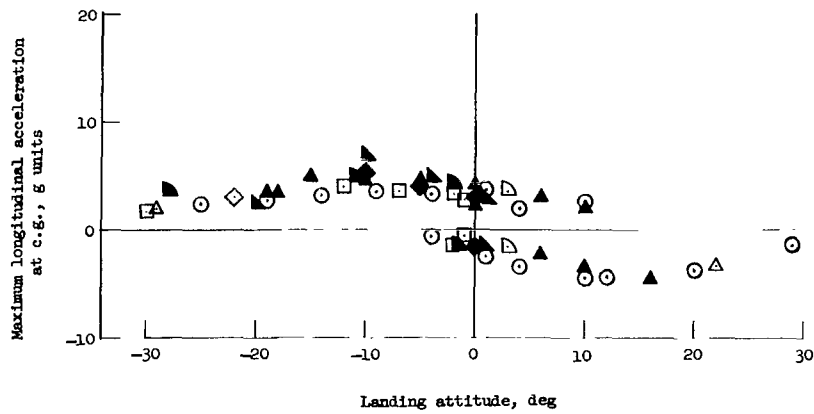
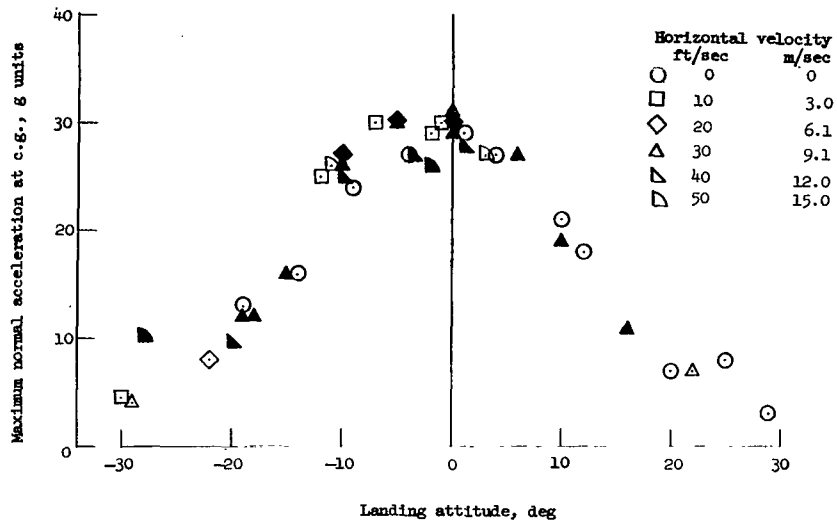


(b) Landing on a sand surface; horizontal velocity, 0.



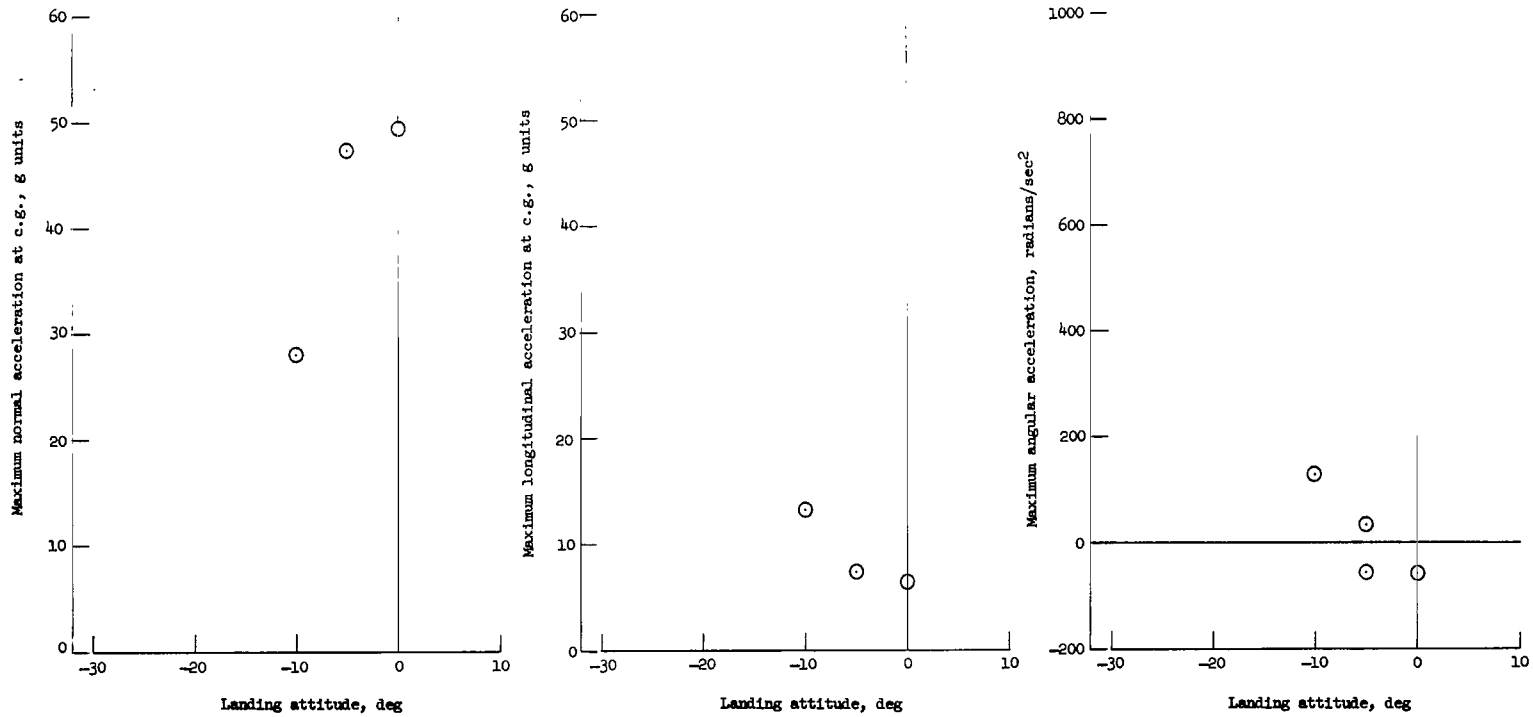
(c) Landing on a hard clay-gravel composite surface; horizontal velocity, 30 ft/sec (9.1 m/sec).

Figure 15.- Typical oscillograph records of accelerations for landings on water, sand, and a clay-gravel composite surface. Vertical velocity, 23 ft/sec (7.0 m/sec); pitch, -10° ; roll, 0° ; yaw, 0° . All values are full scale unless otherwise indicated.



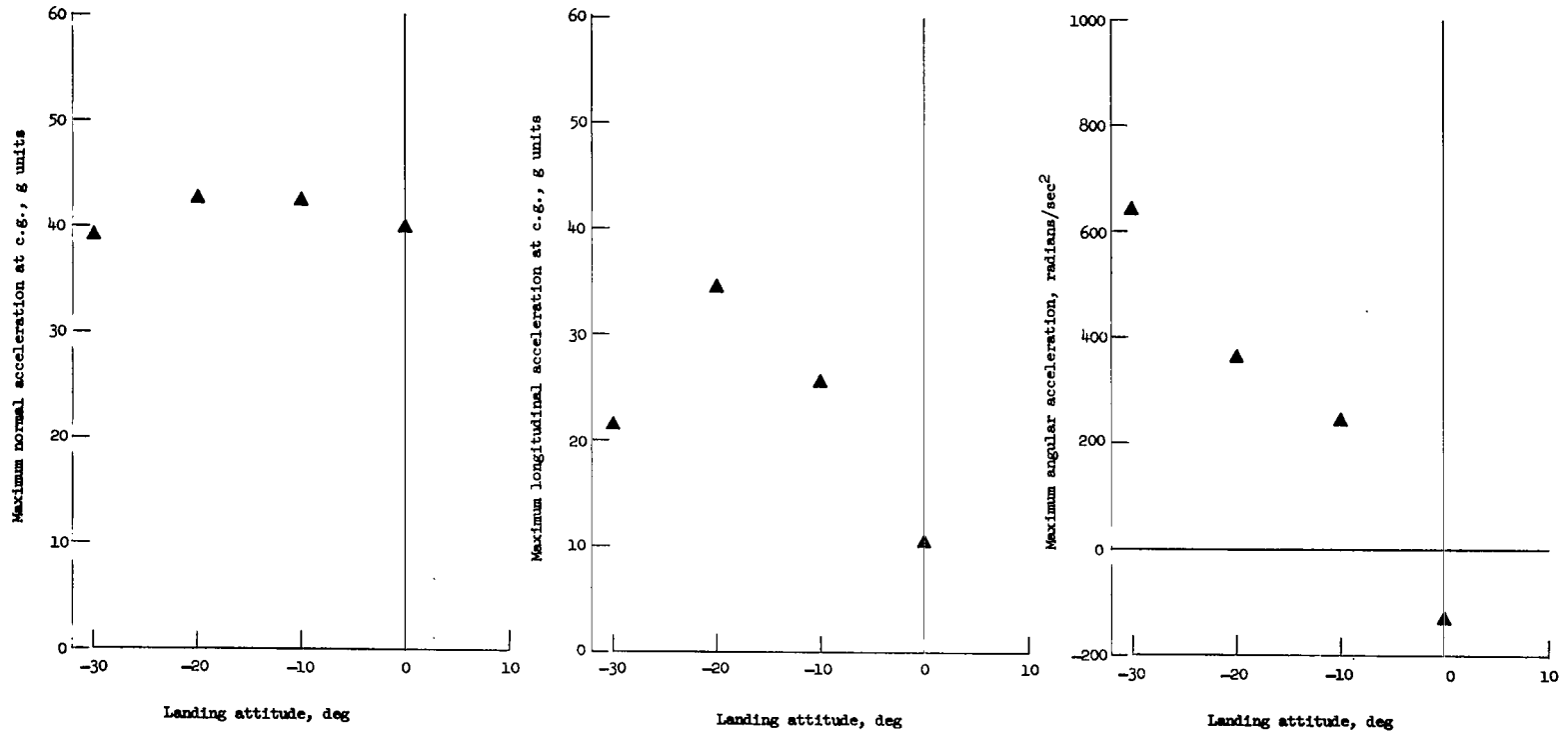
(a) Water landing surface.

Figure 16.- Maximum accelerations for passive landing system. Vertical velocity, 23 ft/sec (7.0 m/sec); roll, 0°. All values are full scale. (Shaded data points indicate turnover.)



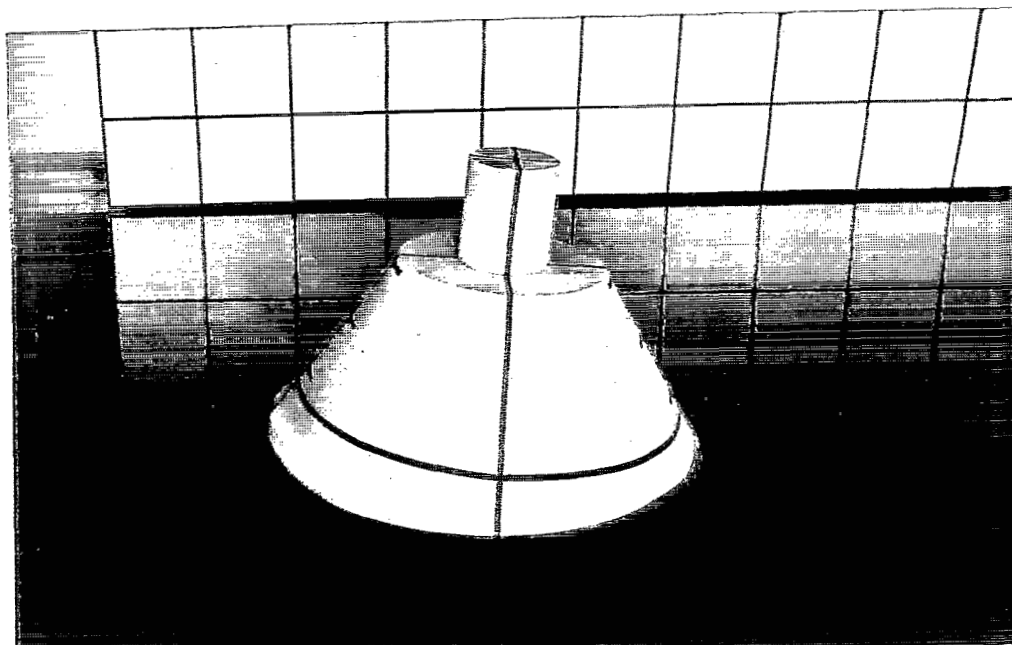
(b) Sand landing surface. Horizontal velocity, 0. Heat-shield failure occurred at landing attitudes of 0° and -5° .

Figure 16.- Continued.



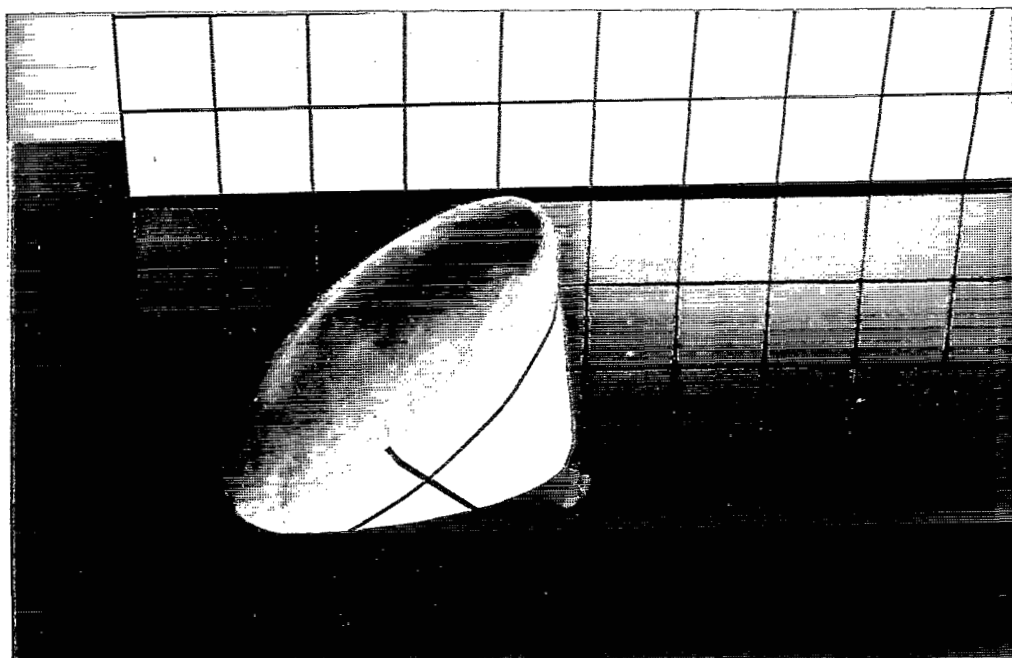
(c) Clay-gravel composite landing surface. Horizontal velocity, 30 ft/sec (9.1 m/sec). Heat shield failed for all tests.

Figure 16.- Concluded.



(a) Stable position floating upright.

L-63-1690



(b) Stable position after turnover.

L-63-1695

Figure 17.- Photographs of vehicle floating in calm water.

A motion-picture film supplement L-960 is available on loan. Requests will be filled in the order received. You will be notified of the approximate date scheduled.

The film (16 mm, 5.7 min, color, silent) shows landing tests of the 1/4-scale model of the Apollo command module made on water, sand, and hard clay-gravel composite landing surfaces using a passive landing system.

Requests for the film should be addressed to:

Chief, Photographic Division
NASA Langley Research Center
Langley Station
Hampton, Va. 23365

CUT

	Date _____
Please send, on loan, copy of film supplement L-960 to TN D-3980	
Name of organization	_____
Street number	_____
City and State	_____ Zip code
Attention: Mr.	_____
Title	_____

"The aeronautical and space activities of the United States shall be conducted so as to contribute . . . to the expansion of human knowledge of phenomena in the atmosphere and space. The Administration shall provide for the widest practicable and appropriate dissemination of information concerning its activities and the results thereof."

—NATIONAL AERONAUTICS AND SPACE ACT OF 1958

NASA SCIENTIFIC AND TECHNICAL PUBLICATIONS

TECHNICAL REPORTS: Scientific and technical information considered important, complete, and a lasting contribution to existing knowledge.

TECHNICAL NOTES: Information less broad in scope but nevertheless of importance as a contribution to existing knowledge.

TECHNICAL MEMORANDUMS: Information receiving limited distribution because of preliminary data, security classification, or other reasons.

CONTRACTOR REPORTS: Scientific and technical information generated under a NASA contract or grant and considered an important contribution to existing knowledge.

TECHNICAL TRANSLATIONS: Information published in a foreign language considered to merit NASA distribution in English.

SPECIAL PUBLICATIONS: Information derived from or of value to NASA activities. Publications include conference proceedings, monographs, data compilations, handbooks, sourcebooks, and special bibliographies.

TECHNOLOGY UTILIZATION PUBLICATIONS: Information on technology used by NASA that may be of particular interest in commercial and other non-aerospace applications. Publications include Tech Briefs, Technology Utilization Reports and Notes, and Technology Surveys.

Details on the availability of these publications may be obtained from:

SCIENTIFIC AND TECHNICAL INFORMATION DIVISION
NATIONAL AERONAUTICS AND SPACE ADMINISTRATION
Washington, D.C. 20546